Check for updates

Landslide Induced Tsunami Hazard at Volcanoes: the Case of Santorini

Ocal Necmioglu,[1,2] (iD) Mohammad Heidarzadeh,[3] (iD) Georgios E. Vougioukalakis,[4] (iD) and Jacopo Selva[5,6] (iD)

Abstract—The destructive tsunami on 22 December 2018 due to the flank collapse of the Anak Krakatau volcano was a bitter reminder of large tsunami risks and of the shortcomings of the existing tsunami warning systems for atypical sources (tsunamis generated by non-seismic and complex sources). In the Mediterranean, several tsunamis were generated by landslides associated with volcanic systems in the past. The volcanic unrest experienced in 2011–2012 on the Santorini volcanic island in the Southern Aegean Sea pointed out the need to identify and quantify tsunami hazard and risk due to possible flank instability which may be triggered as a result of volcanic unrest or nearby seismotectonic activities. Inspired from this need, in this study we examined three possible landslide scenarios in Santorini Island with tsunamigenic potential. The results show that the scenarios considered in our study are able to generate significant local tsunamis impacting Santorini and the nearby islands, as well as producing significant impact along the coasts of the Southern Aegean Sea. While maximum tsunami amplitudes/arrival time ranges are 1.2 m/30-90 min for locations in the Greek-Turkish coasts in the far field, they are in the order of ≈60 m/1-2 min for some locations at the Santorini Island. The extreme tsunami amplitudes and short arrival times for locations inside the Santorini Island is a major challenge in terms of tsunami hazard warning and mitigation. As an effort to address this challenge, a discussion on the requirements for local tsunami warning system addressing atypical sources in the context of multi-hazard disaster risk reduction is also provided.

Keywords: Santorini, Aegean sea, Greece, Volcano, Landslide, Tsunami.

[1] European Commission, Joint Research Centre (JRC), Ispra, Italy. E-mail: ocal.necmioglu@ec.europa.eu
[2] Kandilli Observatory and Earthquake Research Institute, Boğaziçi University, Istanbul, Turkey.
[3] Department of Architecture and Civil Engineering, University of Bath, Bath BA2 7AY, UK.
[4] Hellenic Survey of Geology and Mineral Exploration, Athens, Greece.
[5] Dipartimento di Scienze della Terra, dell'Ambiente e delle Risorse, Università degli Studi di Napoli 'Federico II', Naples, Italy.
[6] Istituto Nazionale di Geofisica e Vulcanologia, Sezione di Bologna, Bologna, Italy.

1. Volcano-Induced Tsunamis: Rare but High-Impact Events

Flank instability and sector collapses are characteristics of all volcanic islands (e.g., Selva et al., 2019, 2020). Data collected from around the world show that volcano-induced tsunamis have caused damage and loss of lives historically: around 130 events from 80 different volcanoes have ben recorded since 1600 AD (Walter et al., 2019; Paris et al., 2014; Paris, 2015; NGDC/WDS Global Historical Tsunami Database, https://www.ngdc.noaa.gov/hazard/tsu_db.shtml). These events have been caused by multiple sources, including the entry of pyroclastic flows into the ocean (De Lange et al., 2001; Carey et al., 1996; Freundt, 2003) and their submarine continuation (Sigurdsson et al., 1991), caldera collapses (Geshi et al., 2017), and landslides entering the ocean (Kelfoun et al., 2010; Krastel et al., 2001; Ward & Day, 2003), or combinations thereof (Nishimura, 2008; Paris, 2015; Paris et al., 2014). Also in the Mediterranean, a significant part of the available catalog (Maramai et al., 2014) include a large number of events with a non-seismic origin, including volcanic events generated in the Gulf of Naples by Mount Vesuvius and in the Aeolian archipelago by Stromboli and Vulcano (Maramai et al., 2005; Selva et al., 2021). The Mediterranean Sea has a long history of atypical tsunamis due to earthquake-triggered submarine landslides, such as the 1908 Messina Strait (Barreca et al., 2021; Favalli et al., 2009; Fu et al., 2017) and the 1956 Amorgos events (Beisel et al., 2009; Okal et al., 2009), and volcanic tsunamis, such as the 2002 Stromboli event (Bonaccorso et al., 2003; Tinti et al., 2006). The relevance of this type of hazard is introduced by discussing below some important aspects of a few case studies.

The recent sector collapse at Anak Krakatau volcano in the Sunda Strait on 22 December 2018 triggered a tsunami that resulted in 437 fatalities. Investigations revealed that prior to its collapse, even though not considered to be as unusual (Perttu et al., 2020), the activity of the volcano had increased, accompanied with thermal anomalies and increase of the surface area of the island, followed by the gradual seaward motion of the southwestern flank on a dipping décollement, showing the importance of a multi-parametric monitoring of volcanoes for tsunami risk mitigation. The collapse of the volcano's flank occurred only two minutes after a small earthquake (Walter et al., 2019), generating a landslide on the southwestern flank of the actively erupting volcano Anak Krakatau. A landslide with a volume of $< \sim 0.2$ km^3 estimated from synthetic aperture radar and broadband seismic observations, has been considered as the source of the tsunami (Ye et al., 2020). Dogan et al. (2021) hypothesized a flank collapse scenario with a volume of 0.25 km^3 as a combination of submarine and subaerial mass movement as the best scenario for the source mechanism capable of explaining the observed coastal amplitudes, but subject to uncertainties in the numerical modeling due to rheology of the collapsed material, the reflection effects of coastal topography, and the role of coastal protection, including coastal forest in modeling. Two different source models with volumes of 0.175 km^3 and 0.326 km^3 presented by Heidarzadeh et al., (2020a, 2020b) were also able to explain the observations. It's noteworthy that the event was successfully hypothesized already in 2012 by Giachetti et al. (2012). Other successful modeling of the 2018 Anak Krakatau volcanic tsunami were conducted by Grilli et al., (2019, 2021) and Zengaffinen et al. (2020).

It is long argued that based on geologic evidence, a future eruption of the Cumbre Vieja Volcano on the Island of La Palma may trigger a catastrophic failure of its west flank, dropping 150 to 500 km^3 rock into the sea, resulting in a tsunami in the Atlantic Basin with a speed of 100 m/s and impacting the coasts of Americas with 3–8 m in Newfoundland (Canada) and 10–25 m (Florida, USA) height, respectively (Ward & Day, 2001). Significant wave impact has been modeled in near- and far-field even for reduced source volumes (Abadie et al., 2012, 2020), where it is claimed that La Palma, the town of Santa Cruz, would be struck by two simultaneous inundation waves with devastating consequences and important cities in Gran Canaria or Tenerife were identified as subject to high tsunami impact for every considered scenario. It's important to note, however, that another study (Pararas-Carayannis, 2002) rejects such claims.

From the early twentieth century, Stromboli generated at least six tsunamis (Maramai et al., 2005, 2014). In Stromboli, tsunamigenic landslides originated at the Sciara del Fuoco (SdF), along the eastern coast of the island (Tinti et al., 2005). Such landslides may be triggered by paroxysmal eruptions, with tsunamis occurring a few minutes after the explosion, but may also be triggered during effusive phases (Di Traglia et al., 2014; Ripepe et al., 2021; Selva et al., 2021; Valade et al., 2016). The most recent significant event in this region occurred on 30 December 2002, with a run-up along the island of more than 10 m. Also, this event was generated by a landslide at SdF, and a detailed reconstruction of the events and numerical computations of landslide and tsunamis are provided by Tinti et al., (2005, 2006). Such repeated events pushed the authorities to develop a local tsunami warning system for tsunamis generated at the SdF, which has been recently tested with two minor tsunami events in 2019 (Selva et al., 2021 and references therein).

The large volcanic eruption on 15 January 2022 on the Hunga Tonga-Hunga Ha'apai underwater volcano resulted in a tsunami considered to be most likely due to both the collapse of the caldera beneath the sea-level and the air–water coupling generated by the explosion (e.g., Heidarzadeh et al., 2022). The atmospheric shock wave from the explosion generated a tsunami triggered by acoustic-gravity waves (Omira et al., 2022b) reaching the Atlantic Ocean and Mediterranean, where up to 40 cm wave heights have been observed. Significant tsunami waves have been reported in the Pacific Ocean. Locally, this tsunami recalls the large tsunami of the Tongatapu island in the mid-fifteenth century with runup heights up to 30 m. The source of the associated tsunami was hypothesized as a caldera-forming eruption that would have caused the total collapse of the existing volcanic island located along the Tonga ridge less

than 150 km southwest off Tongatapu (Lavigne et al., 2021). Similar effects were observed during the 1883 Krakatau eruption (Satake et al., 2020).

2. The Case of Santorini

2.1. Seismotectonic and Geologic Setting of Santorini

The Aegean and its surroundings is the most active part of the Africa–Eurasia collision zone characterised with the high level of seismicity (Moratto et al., 2007; Papazachos, 1990) as a result of the compressional motion between the European and African plates and associated tectonic processes such as subduction of the eastern Mediterranean lithosphere along the Hellenic Arc under the Aegean and the westward motion of the Anatolian Block along the North Anatolian Fault (McKenzie, 1970; Moratto et al., 2007). The whole Aegean Back Arc is mainly dominated with normal faults (McKenzie, 1978; Moratto et al., 2007), whereas the low-angle thrust faults along the Hellenic arc accommodates the dense shallow seismicity (Moratto et al., 2007; Necmioglu & Ozel, 2015; Papazachos, 1990).

The crustal deformation in the Aegean backarc has localized progressively during slab retreat from Late Eocene to present and the extension is localized in Western Turkey, the Corinth Rift and the external Hellenic arc after Messinian times. The direction and style of extension have not changed considerably through the time, except in terms of localization. The fundamental element of the driven tectonic regime is the slab retreat, where successive slab tearing episodes are the main causes of strain localization, and heterogeneity of the crust is a major factor for localized detachments. The strain localisation in the upper plate is also influenced by the dynamics of slabs at depth and the asthenospheric flow due to slab retreat (Jolivet et al., 2013).

The South Aegean Volcanic Arc (SAVA) (Fig. 1) is composed of five volcanic fields, as follows: (i) Sousaki, (ii) Saronikos (Aegina, Poros, Methana), (iii) Milos (Milos, Kimolos, Polyegos, Antimilos), (iv) Santorini (Christiana, Santorini, Kulumbo) and (v) Nisyros (Kos, Nisyros, Yali). Eruptions in

historical time have been registered at Methana, Milos, Kamenis, Kulumbo and Nisyros (Vougioukalakis et al. 2019).

Santorini is the most active volcanic system of the SAVA (Vougioukalakis and Fytikas, 2005), extending from Methana peninsula to the west to Nysiros Island to the east (Fig. 1). It presently consists of a small archipelago of five islands, namely Thera, Thirasia, and Aspronisi, which constitute a ring structure bordering the Santorini caldera, and Palea Kameni and Nea Kameni which emerge in the caldera center (Tassi et al., 2013). Two volcanic systems occur along a NE–SW trending tectonic line produced by a NNW–SSE extensional stress regime (Vougioukalakis and Fytikas, 2005; Sakellariou et al., 2010; Dimitriadis et al., 2009), namely, Christiana Islands, 20 km SW of Santorini caldera, and Kolumbo submarine volcano located 8 km NW of Thera, where more than 20 volcanic cones have been identified (Alexandri et al., 2003; Nomikou et al., 2012; Vougioukalakis et al., 1994, 1995). SAVA has formed in response to the subduction of the African plate beneath the Aegean microplate (Francalanci et al., 2005; Le Pichon & Angelier, 1979; McKenzie, 1972; Papazachos & Comninakis, 1971; Tassi et al., 2013). Santorini experienced more than a hundred explosive eruptions and at least four caldera collapses in the last 400,000 years (Tassi et al., 2013; Druitt et al., 1989; Druitt and Francaviglia, 1992), with nine major eruptions in the last 600 years (Fytikas et al., 1984; Georgalas, 1962; Tassi et al., 2013). Based on synchronizing Santorini's stratigraphy with the sea-level record using tephra layers in marine sediment cores, Satow et al. (2021) showed that the large majority of the eruptions occurred during periods characterised by sea-level falls of > 40 m and subsequent rises, suggesting a strong correlation between the eruptions of the Santorini and the sea-level change. Recent studies even suggested that the seasonal rainfalls can significantly weaken volcanoes as a result of pore-pressure build-up leading to dyke intrusion and eventually triggering the eruptive cycle (Sahoo et al., 2022).

The Santorini caldera formed from the huge Minoan explosive eruption occurred around 1600 BC (Bond & Sparks, 1976; Druitt et al., 2019; Friedrich, 2000; Heiken & McCoy, 1984; Pyle, 1990;
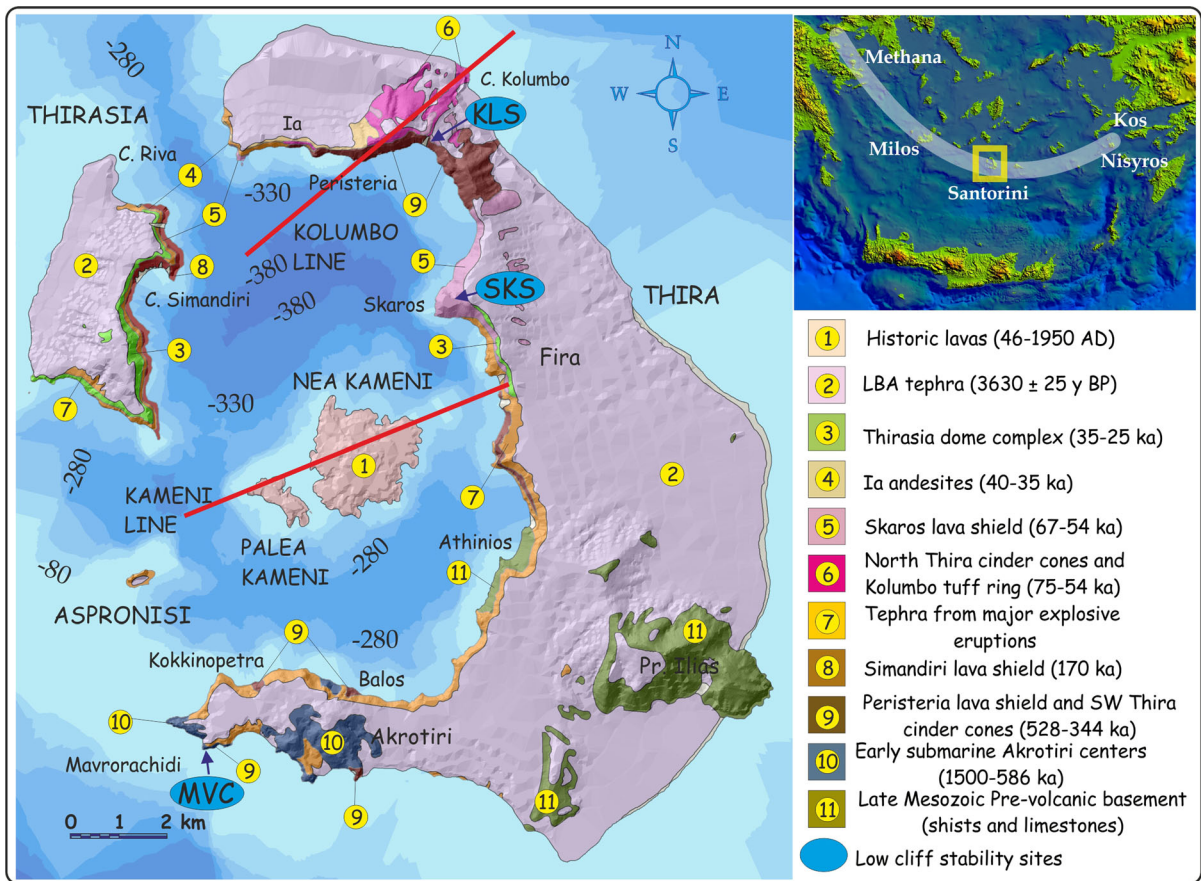
Figure 1
Geologic setting of the Santorini, water depth contours and locations of possible instabilities identified in this study

Sparks & Wilson, 1990; Tassi et al., 2013), along the so-called Kameni tectonic line (Fytikas et al., 1990; Tassi et al., 2013). After the Minoan eruption, two volcanic islets (Palea and Nea-Kameni) formed with a series of smaller eruptions between 197 BC and 1950 AD (Pichler & Kussmaul, 1980; Tassi et al., 2013). The last eruptions occurred at Nea Kameni in 1926, 1940, and 1950 (Georgalas, 1953; Tassi et al., 2013). After that, the volcano has been characterized by several unrest episodes, the last of which occurred in 2011 and was characterized by an intense seismicity and deformations localized in the northern part of the caldera, along a volcano-tectonic line that extends from Santorini to the nearby island of Amorgos (Newman et al., 2012; Parks et al., 2015; Rizzo et al., 2015; Tassi et al., 2013). As a result of this volcanic evolution, present day caldera is mainly

submerged and surrounded by stiff rims characterizing the inner part of the islands of Santorini, which collectively form an almost closed ring around the deep inner bathymetry (Fig. 1).

2.2. Santorini, Largest Known Tsunami Ever in the Eastern Mediterranean

The Plinian eruption of Santorini (Thera, ca. 1600 BC) in the Late Bronze Age, at an estimated Volcanic Explosivity Index (McCoy et al., 2000) equal to 7, was one of the largest eruptions in the history (Carey et al., 2006; Druitt et al., 2019; Friedrich et al., 2006; Manning et al., 2006; McCoy & Heiken, 2000), with an impact on the whole Eastern Mediterranean, confirmed by both sedimentary deposits as far as Caesarea Maritima (Israel) and computer modeling

(Goodman-Tchernov et al., 2009). The volume of the Minoan eruption was in fact hypothesized as to be comparable to that of the largest known historical eruption, i.e., the 1815 eruption of Tambora in Indonesia (Carey et al., 2006; Sigurdsson & Carey, 1989).The most likely mechanism of tsunami generation was the entry of pyroclastic flows into the sea, combined with slumping of submarine pyroclastic accumulations (Nomikou et al., 2016). A landslide deposit of approximately 6 km wide by 20 km long, and up to 75 m thick has been proposed as the source of the tsunami (Bell et al., 2013).

Based on numerical modeling results and distribution of sediments, it has been argued that the seawater flooding due to the tsunami generated by the Santorini eruption in 16th Century BC was restricted to the coastal zone of Crete and all along the Aegean coast, hence the tsunami would have had little influence on Minoan civilization (Minoura et al., 2000). While Dominey-Howes (2004) argues that the paroxysmal Late Bronze Age (LBA) eruption of Santorini probably generated multiple tsunamis with no significant far-field tsunami propagation throughout the entire east Mediterranean as frequently claimed. Şahoğlu et al. (2022) presented articulated human and dog skeleton as archeological evidence discovered within the tsunami debris in a more than 200 km away western Anatolian/Aegean coastal archeological site Çeşme-Bağlararası as in situ victims related to the Late Bronze Age Thera eruption event.

2.3. Santorini Volcanic Unrest 2011–2012

The Santorini Volcano experienced its first seismo-volcanic unrest since 1950 during 2011 and the first half of 2012, which was detected and monitored through permanent networks and a large number of measurement campaigns (Vougioukalakis et al., 2016). An investigation of the geochemical and isotopic changes in the fumarolic and submerged gas discharges during the 2011–2012 unrest at Santorini caldera demonstrated that the geophysical and geochemical signals of this unrest are interrelated (Tassi et al., 2013). A study by Parks et al. (2015) on the quiescence and slow subsidence period during 1993–2010 followed by a phase of unrest during

January 2011 to April 2012 revealed that the optimal location of the inflating source is situated north of Nea Kameni at a depth of $\sim$ 4 km. Two distinct pressure pulses were identified corresponding to volume changes in the shallow magma chamber. This behaviour accounts for the observed temporal variation in cumulative volume change and seismicity after approximately 60 years of seismic quiescence (Newman et al., 2012) throughout the period of unrest (Parks et al., 2015). Seismicity was characterized mainly by small events (Chouliaras et al., 2012). Observations in the southern part of the caldera show that this area remained practically stable during 1994 and 2000 and the partial caldera inflation was related to slow magma intrusion not associated with changes in the seismicity (Stiros et al., 2010).

This unrest led to concerns on the possibility for a volcanic reactivation of Nea Kameni (Aspinall & Woo, 2014), eventually resulting in a tsunami due to the underwater explosions, as well as on the potential tsunamis generated due to possible geotechnical problems along the steep caldera cliffs. This is a huge risk to local communities considering more than 15,000 permanent residents and significant increase in the population during the summer period (Jenkins et al., 2015). Landslides and detachments of large masses were identified as possible origins of small tsunamis, which could threaten the intra-caldera coastline as well as the port of Athinios (Barberi & Carapezza, 2019; Vougioukalakis et al., 2016).

2.4. The Need for a Volcano-Tsunami Hazard Study for Santorini

The assessment of natural hazard plays a critical role in the communication of associated risks to a diverse range of stakeholders (Charlton et al., 2020). In volcanic systems, hazard and impact assessments from volcanic eruptions are widely exploited by disaster risk reduction agencies, emergency managers and civil protection authorities, but only a few of them address also the non-eruptive volcanic hazards (Charlton et al., 2020; Hayes et al., 2020; Kaye et al., 2009; Selva et al., 2019, 2020; Zuccaro et al., 2008). Episodes of volcanic unrest, similar to the Santorini volcanic unrest during 2011–2012, may be connected

to many hazards, including tsunamis. During unrest, the likelihood of tsunamigenic landslides is indeed increased by, for example, deformations, seismic activity, or alteration of materials due to intense degassing (e.g., Selva et al., 2020). Unrest episodes are observed at each year in about 20 large calderas (Acocella et al., 2015; Charlton et al., 2020; Newhall & Dzurisin, 1988), which can continue for years or more (Charlton et al., 2020; Phillipson et al., 2013; Potter et al., 2015) and may have a considerable impact on the local and regional economies (Barberi et al., 1984; Charlton et al., 2020; Johnston et al., 2002; Longo, 2019; Potter et al., 2015). Notably, also moderate-scale events might have cascading, catastrophic effects, mainly due to the modern-day clustering of critical infrastructures in the vicinity of active volcanic regions (Mani et al., 2021).

There are very few studies on present day tsunami hazard in Santorini. An assessment of building vulnerability to tsunami hazard in Kamari on Santorini Island, based on a worst-case run-up scenario of 10 m above sea-level tsunami generated due to a Mw $\sim$ 8.5 earthquake in the Hellenic Arc, indicated that more than 400 buildings would be within the inundation zone, where more than half of them were identified as highly-very highly vulnerable to tsunamis (Batzakis et al., 2020). Based on seismic studies indicating highly active region beneath Kulumbo submarine volcano as potential future eruptive activities, Nomikou et al. (2014) considered generation of tsunami based on submarine slope collapses due to volcanic and volcano-triggered seismic activity and concluded that, compared to the 1650 AD Santorini event, the magnitude of explosive eruptions from Kulumbo is likely to be much smaller but the proximity of the volcano to the eastern coast of Santorini makes it exposed to significant risks even for low-magnitude events. Kazantzidou-Firtinidou et al. (2018) suggested to consider secondary seismic effects (such as slope instabilities, rock falling, tsunamis or tephra fallouts) for future multi-hazard analysis. It should be emphasized that while Aegean volcanoes and Santorini in particular represent a significant volcano-related tsunami hazard, the hazard may have an important directional component depending on the eruption mechanism, in the sense that a future volcanic origin tsunami may affect specific coasts in certain directions only (Dominey-Howes, 2004), as demonstrated through the modeling results presented later in this manuscript.

3. Modeling Results of Possible Instabilities as a Result of Increased Degree of Unrest or a Major Earthquake Nearby

Sediment failures in the Santorini (Thera) Basin in the Aegean Sea are mainly associated with the seismic activity and seismicity related to modern volcanic activity, steep slopes, and the open sediment structure due to the specific texture of the volcanic material (Hasiotis et al., 2007). Tsunami hazard quantifications, as for all natural hazards, should in principle consider the full variability of the potential sources, in order to provide a complete picture of what can happen in the future. This task is typically pursued with Probabilistic Tsunami Hazard Analyses (PTHA), which provide a framework to quantify the probability that a given tsunami intensity measure (e.g., maximum run-up height) is exceeded at a particular location within a given time period due to a given source (Grezio et al., 2017; Heidarzadeh & Kijko, 2011). For volcanic and landslide sources, this task is particularly hard, mainly due to the diversity of potential sources and the difficulties in constraining their recurrence rates (Behrens et al., 2021; Løvholt et al., 2020; Paris, 2015; Selva et al., 2021; and references therein). While the quantitative definition of the hazard remains the final goal, a viable first step toward the definition of the tsunami hazard is the quantification of the potential tsunami threat posed by a reasonable range of possible sources. This deterministic approach simplifies the treatment of source variability and recurrence rates and it provides a first order quantification of the potential variability of the tsunami threat based on past events and present knowledge of the system. This may indeed provide first indications about how the threat can be dealt with, especially for planning potential actions in case of volcanic unrest (e.g., Selva et al., 2019, 2020), and may help prioritizing actions for subsequent detailed PTHA studies.

According to the slope stability analysis in a multi-hazard eruption scenario at the Santorini

volcano by Forte et al. (2019), slopes located in the southeastern part of the island represent the pre-volcanic relief of Thira. Inner slopes of the Thira caldera, located all along the western perimeter of the island, show a typical stepped profile due to the interbedding of strata made up by hard (generally lavas) and soft pyroclastic rocks and have the highest gradients (> 30°). These slopes always show an active coastal cliff at the base and can reach up to tens of meters high. These units are subject to different gravitational processes such as mechanical wave erosion, rock falls, toppling, and debris flows. In the northeastern and southwestern part of Thira, outer slopes are characterized with mean gradients between 20 and 30° and regular longitudinal profiles, associated with volcanic clusters, mainly formed by lavas, and are generally stable. Lowest gradient slopes (< 20°) are observed in the remaining parts of the outer slopes of the Thira caldera with very irregular planar shapes and profiles, and are generally not affected by major landslide phenomena due to the low gradient (Forte et al, 2019).

In addition to the slope instabilities originated by the various degrees of unrest on Santorini itself, nearby major earthquakes may also have the potential to trigger a landslide on the Santorini. In this regard, it's important to recall that Okal et al. (2009) demonstrated that the observed run-up values of the 9 July 1956 Amorgos M7.8 earthquake, can only be explained by a series of landslides triggered by the mainshock or its main aftershock with M7.2). This hypothesis was further corroborated by Beisel et al. (2009) based on a spectral analysis of the tsunami signal recorded in the port of Yafo, Israel.

3.1. Data and Methods

In the frame of the present morphological, stratigraphic, volcanological and tectonic features of the Santorini volcanic field, we examine three possible scenarios on sites which can be considered as potential sources of landslides which could trigger tsunamis, namely Skaros shield (SKS) and Kulumbo line scarp (KLS), which have been associated with high landslide risk by Antoniou et al. (2017) and Mavro Vouno cone (MVC), which have been associated with low landslide risk by the same study

(Fig. 2). In case SKS, the prominent unconformity is the very steep cliffs of paleocalderas exposed along the present caldera cliffs, covered by scree deposits laying in conformity with the paleo-caldera cliff. The rock masses that could move as a landslide are the post-paleocaldera volcanic products (lava flows and volcaniclastic deposits, which fill the paleocaldera depression with sub-horizontal to gentle slopes inward to the present caldera depression. KLS is the area of the present caldera cliff which has been dissected by a dense vertical or sub-vertical dyke system and the most active present fault system of Santorini area, the so-called "Kulumbo line". In this case we should also take into consideration that this area is considered a "not successful" attempt of a sector collapse during the Minoan caldera forming eruption (Druitt et al., 1999). MVC is the remnant of an eccentric tuff cone edifice, built up along a fault system in the early stages of Santorini volcano activity ($\sim$ 0.53 to 0.35 Ma) by andesitic magmas, on the present steep coastline of South Thira, laying against the Akrotiri submarine tuff and tuffite deposits (Fig. 2). The main idea is to cover the potential variability on spatial initial position and on the potential size of landslides, still directly connecting to realistic scenarios, including source areas both inside (SKS, KLS) and outside (MVC) the caldera (Fig. 1). Thus, each scenario represents a category of a different instability factor that is present on the Santorini Volcanic field and generally in most of the caldera volcanoes edifices.

Table 1 gives the details of the potential subaerial landslides generated by the selected volcanic sources, where the length, width and thickness of the rock volumes, which are in clear discordance or instability, are reported for the selected three areas. Length and thickness of the rock volume has been measured by a laser meter in the field, while the width has been estimated from geological cross sections in a 1:5000 scale geological map. The largest landslide is expected from SKS with estimated length, width and volume of 1000 m, 450 m and 135,000,000 m^3, respectively (Table 1). These landslides are possible following intensive volcanic or volcanic origin seismic activities in the region. Notably, this list does not pretend to be exhaustive in describing potential landslide units in Santorini, and many other potential

sources may be identified. However, as noted above, the three selected sources have been selected rather far to each other and both inside and outside the caldera, so collectively cover a wide range of possible sources.

For modeling landslide tsunamis, we consider a static source for the landslide tsunami, which means the dynamic generation phase of the landslide is simplified. Several authors have applied this method for modeling landslide tsunamis in the past (Heidarzadeh & Satake, 2017; Okal & Synolakis, 2004; Synolakis et al., 2002; Tappin et al., 2008). A major challenge in modeling subaerial landslide tsunamis is estimating the dimension and amplitude of the initial waves generated by landslides (Fritz et al., 2004; Heidarzadeh et al., 2020a, 2020b; McFall & Fritz, 2016; Pranantyo et al., 2021). Here, we assume that the initial wave generated by the subaerial landslides due to volcanoes has a Gaussian shape and thus we consider two parameters for the initial waves comprising maximum initial wave amplitude (A_i) and the initial length of the sea-surface displacement (L_i); subscript "i" is used to mark the initial waves (Fig. 3a).

For estimating these two parameters (A_i and L_i), multiple physical modeling efforts have been performed in the past and several empirical equations were proposed. In this study, we apply two empirical equations proposed by Fritz et al. (2004) and McFall and Fritz (2016) for subaerial landslide tsunamis as well as the rule of thumb developed by Heidarzadeh et al. (2020a). Based on their numerical modeling scenarios, Heidarzadeh et al. (2020a) proposed that the initial wave amplitude can be approximated as half of the landslide thickness and the initial sea-surface displacement length as twice of the landslide length. The empirical equation by Fritz et al. (2004) is as follows:

$$\frac{A_i}{h} = 0.25 \left(\frac{v_s}{\sqrt{gh}}\right)^{1.4} \left(\frac{s}{h}\right)^{0.8} \tag{1}$$

$$\frac{\lambda_1}{h} = 8.2 \left(\frac{v_s}{\sqrt{gh}}\right)^{0.5} \left(\frac{V_s}{bh^2}\right)^{0.2} \tag{2}$$

where, A_i is the maximum initial wave amplitude, λ_1 is wavelength at the relative distance of $\frac{x}{h} = 5$, h is water depth at the landslide source region, v_s is landslide centroid velocity, V_s is landslide volume, g

Figure 2
Generic views of Skaros shield (SKS-left), Kulumbo line scarp (KLS-middle), and Mavro Vouno cone (MVC-right) considered for the tsunami modeling in this study

Table 1

Locations and dimensions of three subaerial landslides in the Santorini islands region that are considered for tsunami modeling

Landslide name (acronym)	Longitude (°E)	Latitude (°N)	Length (m)	Width (m)	Thickness (m)	Landslide volume (m³)
Skaros shield (SKS)	25.417	36.432	1000	450	300	135,000,000
Kulumbo line scarp (KLS)	25.412	36.462	150	60	200	1,800,000
Mavro Vouno cone (MVC)	25.363	36.354	500	600	100	30,000,000

a) Sketch showing initial tsunami source parameters
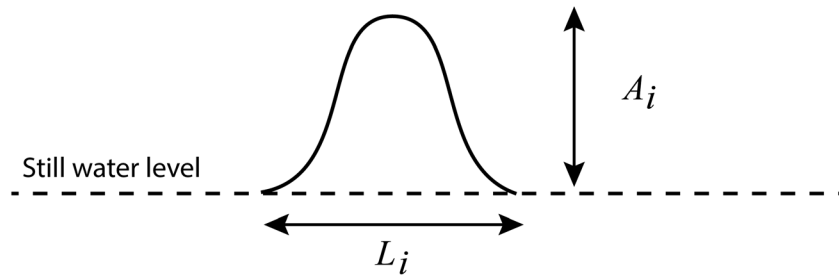
b) Initial wave amplitude of landslide tsunami sources (m)

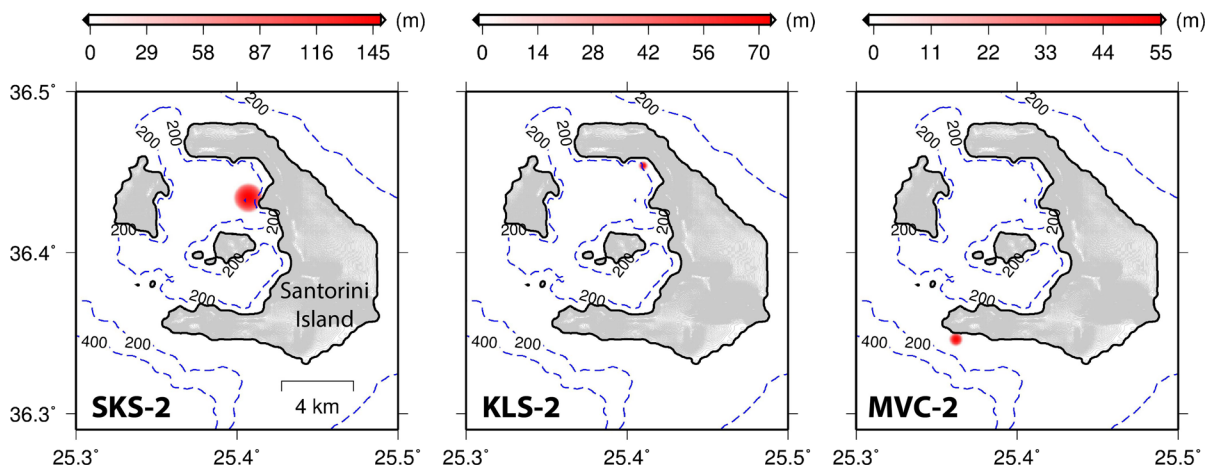

Figure 3

a Sketch showing the two parameters of the initial tsunami source comprising initial landslide-generated wave amplitude (A_i) and the initial length of sea-surface displacement (L_i). **b** Examples of initial tsunami sources used in this study for modeling potential tsunamis. The full list of nine landslide sources is given in Table 3; here, only three of them are shown

is gravitational acceleration, s is landslide thickness, and b is landslide width. As wavelength (λ_1) is usually twice the initial length of the sea-surface displacement (L_i), here we assumed: $Li = 0.5\lambda_1$. As the other empirical equation proposed by McFall and Fritz (2016) is lengthy, we refer the readers to the original article.

Table 2 presents the results of initial wave calculations based on the aforesaid empirical equations. The results of the calculated A_i and L_i vary in a range and thus are associated with some uncertainties, as in all empirical equations (Table 2). Therefore, the parameter ranges are considered in this study for numerical simulations. In order to include such uncertainties in our modeling efforts, we considered three tsunami scenarios for each of the

three landslides and thus modeled a total number of nine tsunami scenarios (Table 3). Figure 3b shows three of these landslide source scenarios. It is noted that the initial amplitudes of the landslide tsunamis listed in Tables 2, 3 may appear unusually large at the first sight; however, they are likely to represent the reality given our recent understanding achieved through the 2018 Anak Krakatau volcanic tsunami, whose initial amplitude was estimated at around 100 m (Grilli et al., 2019, 2021; Heidarzadeh et al., 2020a) and was confirmed through near-field runup surveys by Borrero et al. (2020).

For tsunami modeling, we used the numerical package COMCOT (Cornell Multi-grid Coupled Tsunami Model) (Wang & Liu, 2006), which solves linear and nonlinear Shallow Water Equations on

Table 2

Estimates of the initial landslide-generated wave amplitude (A_i) and the initial length of sea-surface displacement (L_i) based on different predictive equations

Author[*]	Landslide name (acronym)		
	Skaros shield (SKS)	Kulumbo line scarp (KLS)	Mavro Vouno cone (MVC)
Heidarzadeh et al., (2020a)	A_i= 150 m	A_i= 100 m	A_i= 50 m
	L_i= 2,000 m	L_i= 300 m	L_i= 1,000 m
McFall and Fritz., (2016)	A_i= 126 m	A_i= 88 m	A_i= 34 m
	L_i= 1091 m	L_i= 457 m	L_i= 428 m
Fritz et al., (2004)	A_i= 171 m	A_i= 45 m	A_i= 75 m
	L_i= 2100 m	L_i= 640 m	L_i= 838 m
Parameter ranges	A_i= 126 – 171 m	A_i= 45 – 100 m	A_i= 34 – 75 m
	L_i= 1091 – 2100 m	L_i= 300 – 640 m	L_i= 428 – 1000 m

[*]The study by Heidarzadeh et al., (2020a) provides rules of thumb for predicting A_i and L_i, rather than predictive equations. For applying the equation by McFall and Fritz (2016), we assumed a Froude Number of 2.0 for all landslide cases. While applying the two equations by Fritz et al. (2004) and McFall and Fritz (2016), the initial length of sea-surface displacement (L_i) is assumed to be half of the wavelength obtained from the predictive equations

Table 3

Various subaerial landslide tsunami scenarios considered in this study with different initial landslide-generated wave amplitude (A_i) and the initial length of sea-surface displacement (L_i)

Scenario number	Landslide name (acronym)	Longitude (^{o}E)[*]	Latitude (^{o}N)[*]	Initial wave amplitude (A_i)	Initial sea-surface displacement (L_i)
SKS-1	Skaros shield (SKS)	25.407	36.434	126	1091
SKS-2		25.407	36.434	149	1596
SKS-3		25.407	36.434	171	2100
KLS-1	Kulumbo line scarp (KLS)	25.410	36.454	45	300
KLS-2		25.410	36.454	73	470
KLS-3		25.410	36.454	100	640
MVC-1	Mavro Vouno cone (MVC)	25.362	36.346	34	428
MVC-2		25.362	36.346	55	714
MVC-3		25.362	36.346	75	1000

[*]These longitude and latitude coordinates are different from those listed in Table 1 as these scenarios are for tsunami initial waves in the sea

spherical and Cartesian grids on a nested grid system. The nested bathymetric grids used in this study are based on the GEBCO (The General Bathymetric Chart of the Oceans) digital atlas, which offers bathymetric grids with a spatial resolution of 15 arc-sec (Weatherall et al., 2015). We used a two-level nested grid system with grid spacing of 6 arc-sec (Grid-1 in Fig. 4) and 2 arc-sec (Grid-2 in Fig. 4). The Grid-2 covers the entire Santorini Island and all tsunami sources are located within Grid-2 (Figs. 3, 4). A grid spacing of 2 arc-sec is equivalent to approximately 60 m. This implies that all tsunami sources are represented by at least 10 grid points, which is sufficient for modeling. The time step for our simulations was 0.2 s and the total simulation time was 4 h to ensure that the tsunamis arrive at different coastal sites within the Aegean Sea (Fig. 4). Table 4 shows locations of virtual gauges used to record the simulated waveforms at selected locations within the study area.

It is noted that due to the relatively small dimensions of the subaerial landslide sources (Tables 1, 2), the waves generated by them may not be necessarily classified as long waves, rather they may be a mix of long and intermediate waves (e.g., Heidarzadeh et al., 2014). This implies that the waves may show dispersive and nonlinear behaviors. Nonlinearity of the waves are covered in our simulations,
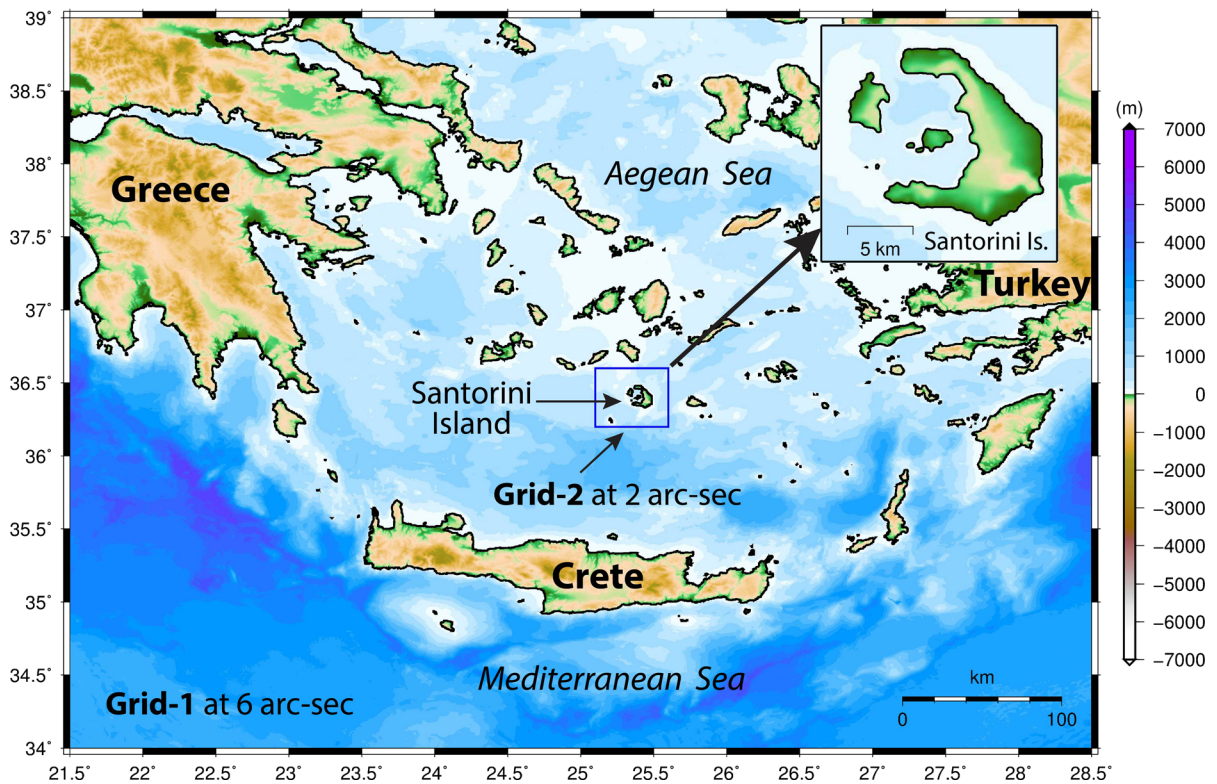
Figure 4

The two-level nested bathymetric grids, with resolutions of 2 arc-sec (the rectangle in the middle) and 6 arc-sec (the entire region except for the area of the rectangle in the middle), used in this study for numerical modeling

Table 4

Locations and water depth of the numerical wave gauges used in this study

Name of the gauge	Longitude (Degree East)	Latitude (Degree North)	Water depth (m)
g1	25.4071	36.4576	50–80
g2	25.3877	36.4583	50–80
g3	23.4242	37.4061	5–15
g4	23.2642	37.3925	5–15
g5	28.3236	37.0387	5–15
g6	27.4400	36.7517	5–15
g7	25.4046	35.3143	5–15
g8	24.4967	35.3724	5–15
g9	25.4758	36.3518	3–5
g10	25.3537	36.3540	3–5

be slightly affected. Such impacts may not be significant as the distance from Santorini to those far-field coasts is less than 200 km (Fig. 5). In addition, dispersion usually has negligible impacts on the maximum amplitudes of the waves although the timing of the peak wave might be slightly shifted due to dispersion. As the purpose of this study is to provide a preliminary estimate of the hazard based on the maximum coastal wave amplitude, the current simulations appear relevant and sufficient as similar modeling have been successfully used in the past (e.g., Heidarzadeh & Satake, 2015; Okal & Synolakis, 2004; Synolakis et al., 2002). For a detailed tsunami hazard analysis of potential Santorini eruptions and associated landslides, we recommend dispersive simulations.

however, dispersion is not included. As a result, the timing of the wave arrivals and number of the waves in the far-field (coasts of Turkey and Greece) might

a) Maximum tsunami amplitudes   **Tsunamis from the Skaros Shield (SKS)**
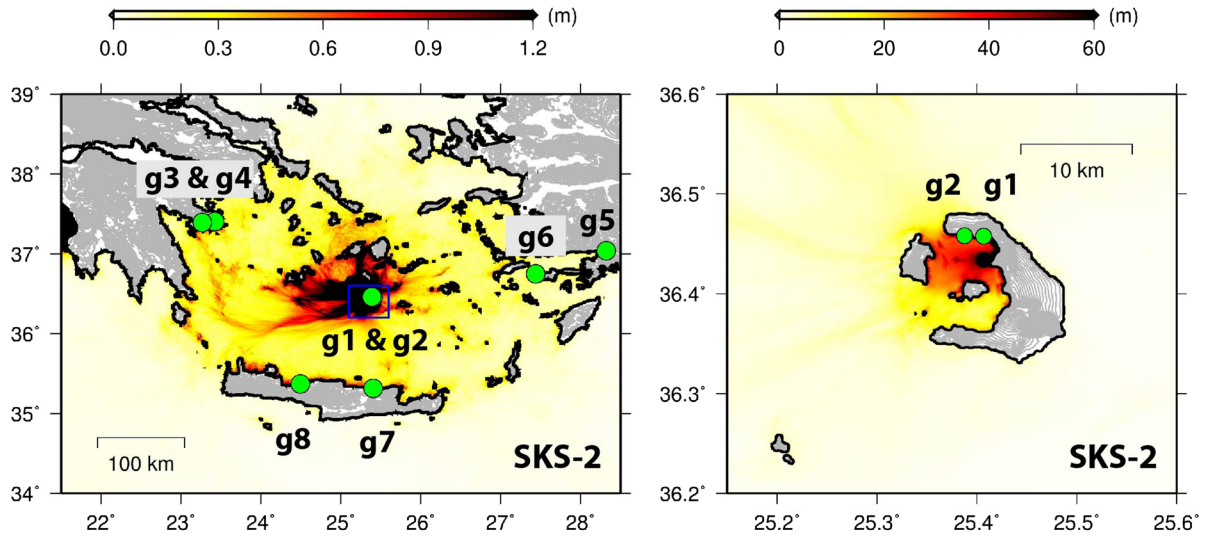
b) Tsunami waveforms from different source scenarios
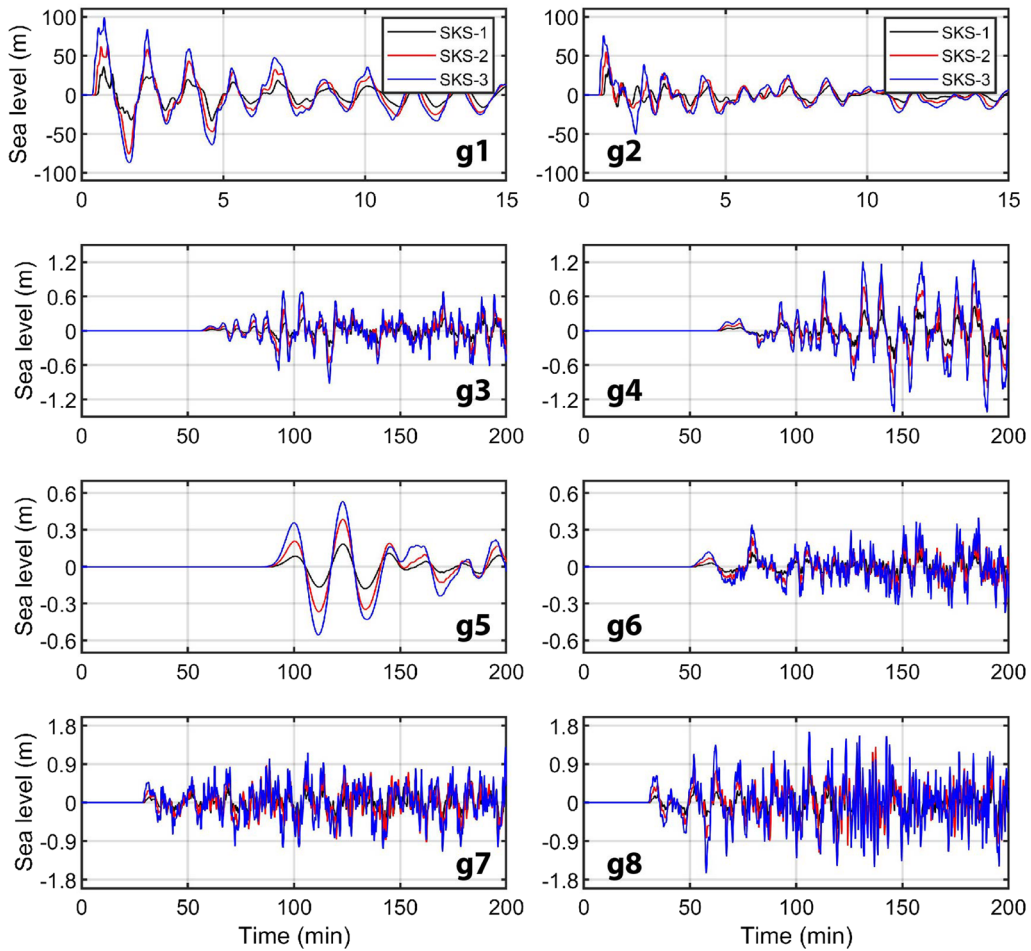
Results of tsunami simulations for the Skaros shield (SKS). **a** Maximum simulated tsunami amplitudes at each grid point during the entire tsunami simulations for the scenario SKS-2. The green circles show the locations of the artificial gauges marked as "g". The area shown by a blue box in the left panel is enlarged in the right panel. **b** Simulated Waveforms from SKS-1, -2 and -3 at different locations

3.2. Results of Simulations

Results of tsunami simulations for Skaros shield (SKS), Kulumbo line scarp (KLS) and Mavro Vouno cone (MVC) are shown in Figs. 5, 6 and 7, respectively. In each of these figures, we show both the maximum simulated tsunami amplitudes during the entire simulation time at each grid point (e.g., Fig. 5a) and the time series of wave oscillations at multiple coastal locations (e.g., Fig. 5b).

For the SKS scenarios (Fig. 5), it can be seen that the scenario SKS-2 generates more than 60 m of tsunami amplitudes within the Santorini Island and export waves larger than 1.2 m to coasts across the Aegean Sea (Fig. 5a). Coastal gauges recorded waves as high as 100 m in the near-field (gauge g1; Fig. 5b). In the far-field, the waves reach amplitudes up to 1.2 m along the Greek coasts (gauges g3 and g4; Fig. 5b), up to 0.5 m along the Turkish coasts (g4 and g5; Fig. 5b), and up to 1.7 m along northern coasts of Crete (g7 and g8; Fig. 5b). It is important to note that tsunami runup heights can be up to a few times larger than the coastal tsunami amplitudes (e.g., Heidarzadeh et al., 2020c). According to Fig. 5a, the scenario SKS-2 generates huge waves with amplitudes 30–60 m in most of the semi-confined area within the Santorini Island. These situations generated by SKS-2 and SKS-3 are similar to those of the near-field areas affected by the December 2018 Anak Krakatau volcano landslide tsunami which experienced maximum runup heights of 80–85 m (Borrero et al., 2020). In the far-field area (coasts of Greece and Turkey), the tsunami amplitudes from the two scenarios of SKS-2 and SKS-3 are considered relatively high and are capable of causing moderate damage. The smallest scenario (SKS-1) generates wave amplitudes of 20–30 m in the near-field whereas the far-field amplitudes are negligible

(Fig. 5b). This indicates that SKS-1 is considered a threat only for areas within the Santorini Island.

The KLS scenarios (Fig. 6) appear to be a threat mostly in the near-field as the coastal amplitudes along the coasts of Greece, Turkey and Crete are below 0.2 m (Fig. 6b). However, in the near field, all three KLS scenarios produce large waves capable of causing significant destruction. The scenario KLS-2 impacts almost all of the Santorini Island's interior coasts with waves larger than 5 m (Fig. 6a) and the northern part of the Santorini interior coasts with waves as high as 20 m (Fig. 6a; gauge g1 in Fig. 6b). The tsunami generated by KLS-1 appears to be high only around the source area (e.g., gauge g1 in Fig. 6b) and is negligible on other coastal locations within the Santorini Island.

The MVC scenarios are different from the SKS and KLS scenarios by their minimum impacts on the interior coastlines of the Island (Fig. 7a). The three MVC scenarios produce small waves in the far-field coasts along the coasts of Greece and Turkey and therefore are not far-field threats, although the waves are noticeable and may generate some lasting wave oscillations inside ports, harbors and bays. In the near-field, the waves generated by MVC-2 are as high as 20 m and thus are considered as major hazards for local communities. The waveform record of gauge g9, resulting from MVC-2 (Fig. 7b), is flattened out at time around 2 min indicating that the gauge is possibly out of water due to tsunami receding.

In terms of tsunami arrival times, the first tsunami peak waves due to the SKS scenarios (Fig. 5) affect the near-field areas within 1–2 min (Fig. 5b). In the far-field, the tsunami arrival times are approximately 60 min at Greek coasts, 55–90 min for Turkish coasts, and approximately 30 min in Crete.

4. Discussion

Our results show that the largest scenario among the selected scenarios due to flank instability in Santorini (i.e., the SKS scenarios), which produce more than 60 m of tsunami amplitudes within the interior coasts of the Santorini Island, can produce a tsunami waves comparable to those of the near-field areas following the December 2018 Anak Krakatau

a) Maximum tsunami amplitudes   **Tsunamis from Kulumbo Line Scarp (KLS)**
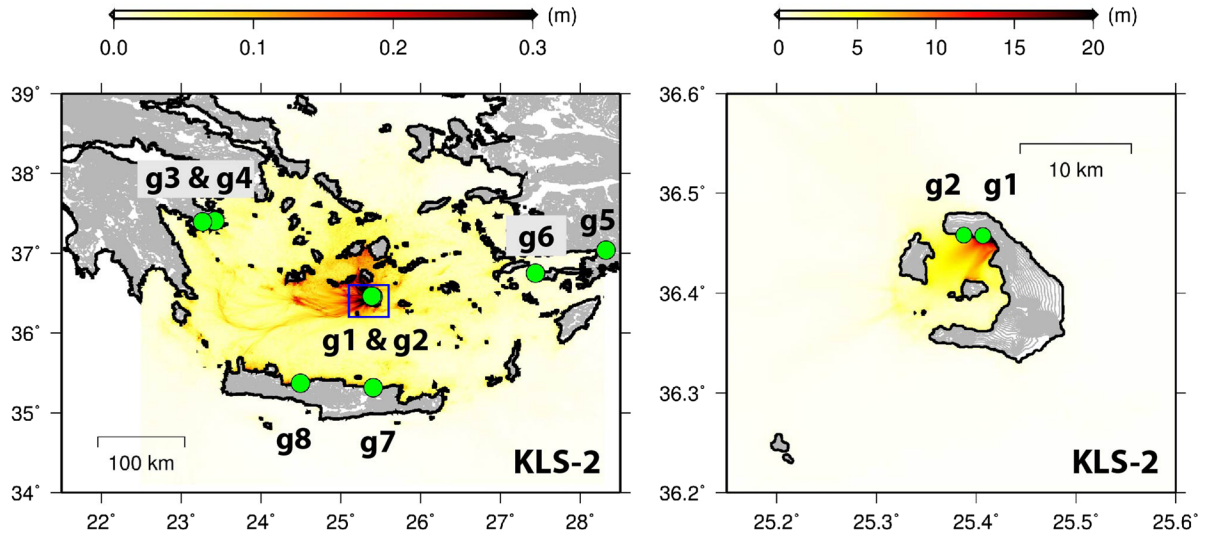
b) Tsunami waveforms from different source scenarios
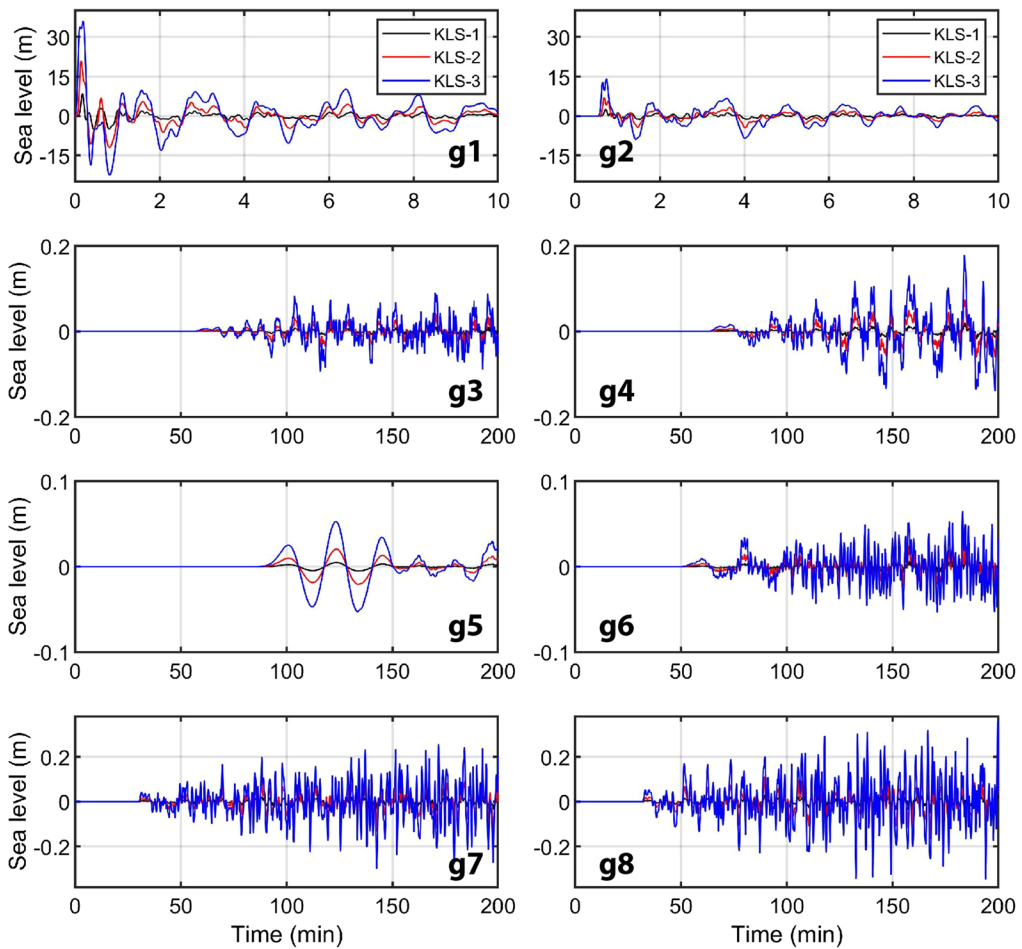
Results of tsunami simulations for the Kulumbo line scarp (KLS).
a Maximum simulated tsunami amplitudes at each grid point
during the entire tsunami simulations for the scenario KLS-2. The
green circles show the locations of the artificial gauges marked as
"g". The area shown by a blue box in the left panel is enlarged in
the right panel. **b** Simulated Waveforms from KLS-1, -2 and -3 at
different locations

volcano landslide tsunami. In the far-field area
(coasts of Greece and Turkey), the tsunami ampli-
tudes can be larger than 1.2 m. In the case of KLS
scenarios, the threat appears to be mostly in the near-
field, with a tsunami capable of causing large
destruction in almost all of the Santorini Island's
interior coasts with waves larger than 5 m, as well as
in the north part of the coast with waves as high as
20 m. Such phenomena could lead to the complete
destruction of the Athinios Ferry Port at the bottom of
the caldera, main port of Santorini, located approxi-
mately 10 km from Fira. Even though the MVC
scenarios result in minimum impact on the interior
coastlines of the Island and negligible waves in the
far-field coasts, the waves can be as high as 20 m in
the near-field and thus should be considered as major
hazards for local communities.

The very large values that we obtain for the
potential heights of local tsunamis should not be
considered surprising. Atypical sources (tsunamis
generated by non-seismic and complex sources) are
indeed responsible for some of the highest measured
tsunami runup (e.g., 524 m of runup due to the 1958
Lituya Bay landslide tsunami) and of the most dev-
astating historical tsunamis, such as the 1883
Krakatau volcano tsunami (Titov, 2021). This clearly
highlights the need, in volcanic islands, of a multiple
hazard mitigation approach that includes tsunamis
(Selva et al., 2019, 2020). The recent 15 January
2022 Tonga event once more demonstrated this need.
Operational Tsunami Early Warning Systems under
the UNESCO-IOC framework are currently limited to
earthquake–generated tsunamis, but efforts are in
place to consider tsunamis from atypical sources (e.g.
volcano, landslides, weather disturbances) in their
operational settings. As highlighted in the aftermaths
of the 2018 Krakatu and the 2022 Tonga events, the

tsunami risks from atypical sources should be
urgently incorporated into the existing tsunami
warning systems and mitigation measures (Necmio-
ğlu et al., 2021; Selva et al., 2021; Titov, 2021). As
stated above, the Mediterranean Sea has a long his-
tory of atypical tsunamis due to earthquake-triggered
submarine landslides, such as the 1908 Messina Strait
(Barreca et al., 2021; Favalli et al., 2009; Fu et al.,
2017) and the 1956 Amorgos events (Beisel et al.,
2009; Okal et al., 2009), and volcanic tsunamis, such
as the 2002 Stromboli event (Bonaccorso et al., 2003;
Tinti et al., 2005, 2006). In addition, the Tsunami
Early Warning Systems (TEWS) in the Mediter-
ranean Sea face the further difficulty that arises from
the proximity of the tsunami sources to the coasts at
risk (De Girolamo et al., 2014; Selva et al., 2021). A
general discussion on the feasibility of Tsunami Early
Warning Systems for small volcanic islands focusing
on warning of waves generated by landslides at the
coast of the island itself is provided in Bellotti et al.
(2009). This is an extremely challenging task as the
tsunamigenic source is located in the proximity of the
coast and therefore the time available for spreading
the alarm is rather short (e.g., less than 5 min). A first
tsunami monitoring system to alert the island popu-
lation was installed at Stromboli after the 2002
tsunami, composed of instruments that monitor
instabilities of the subaerial flank of the volcano
(Casagli et al., 2009) and instruments that measures
the water elevation in order to verify tsunami gen-
eration, concentrating on the tsunami hazard posed by
one specific source, the Sciara del Fuoco (SdF). The
system has been operative since 2003, with signifi-
cant updates through time, and it is now based on a
multi-parametric monitoring network of the volcanic
activity and two elastic beacons located offshore in
front of the SdF (DPC and RS, 2015; Lacanna &
Ripepe, 2020; Selva et al., 2021). This is to date the
only TEWS for atypical sources operating in the
Mediterranean Sea.

To develop a local system, it is fundamental to
have a multi-parametric monitoring system (Selva
et al., 2021). Since not all the landslides/earthquakes
are tsunamigenic, spreading alarms only on the basis
of the measurement of the instabilities may lead to a
large number of false alarms (Bellotti et al., 2009;
Berndt et al., 2009), which would endanger the

a) Maximum tsunami amplitudes   **Tsunamis from Mavro Vouno Cone (MVC)**
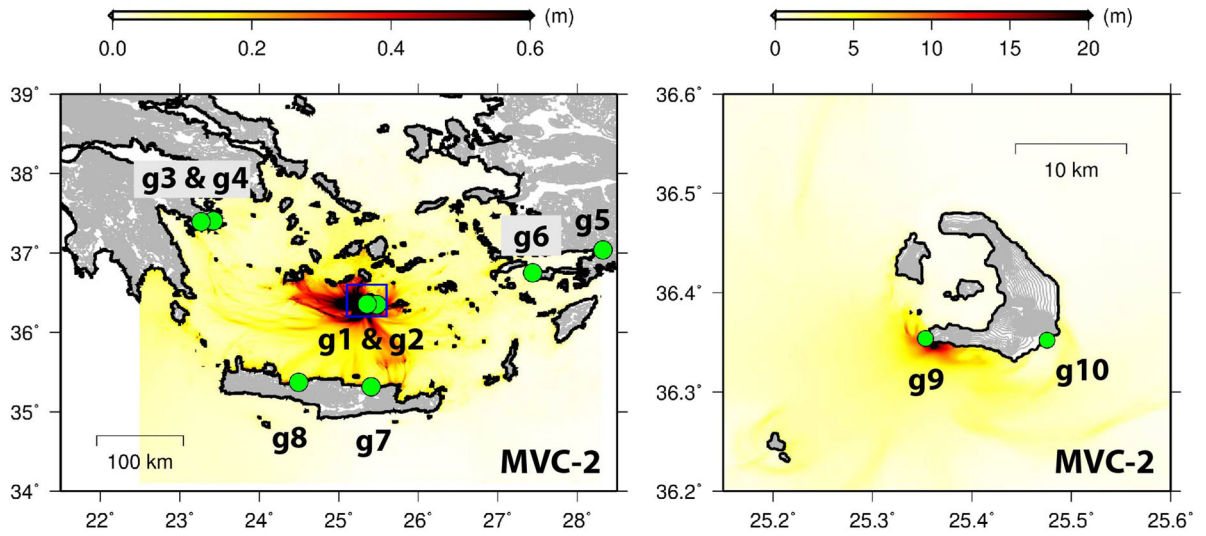
b) Tsunami waveforms from different source scenarios
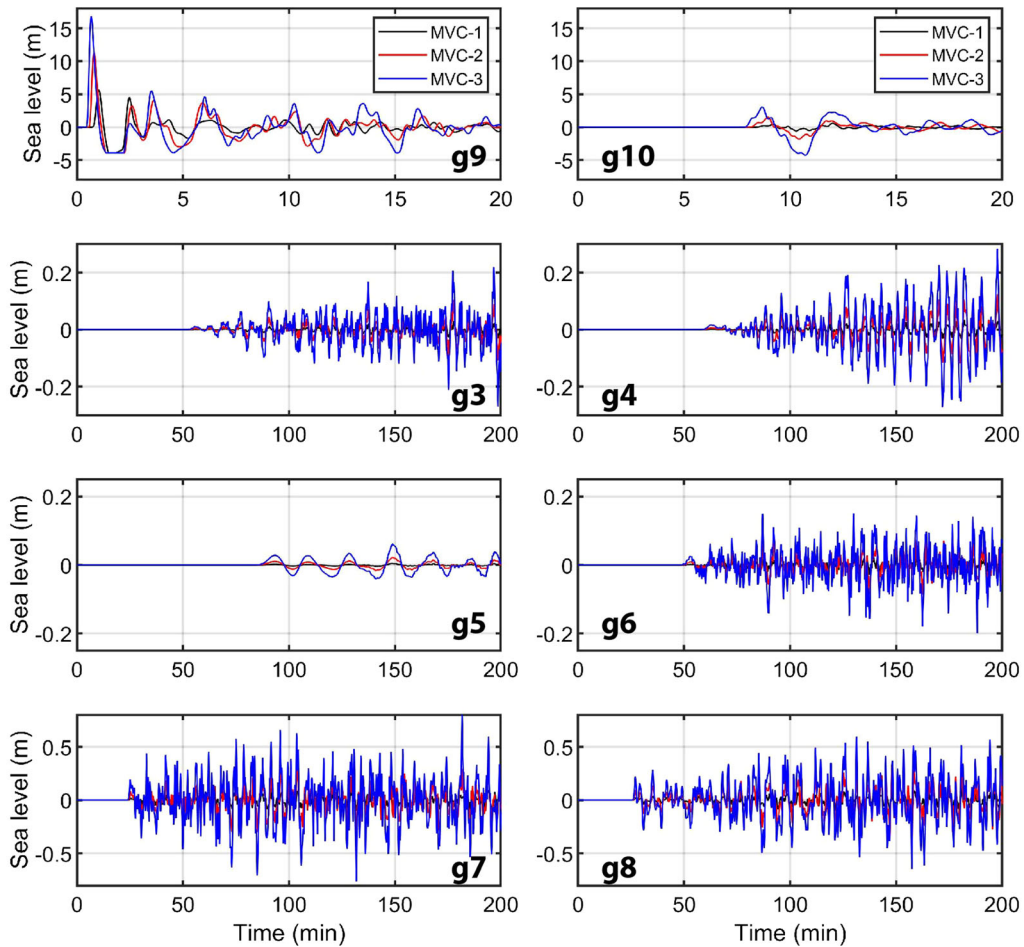
◀Figure 7

Results of tsunami simulations for the Mavro Vouno Cone (MVC). **a** Maximum simulated tsunami amplitudes at each grid point during the entire tsunami simulations for the scenario MVC-2. The green circles show the locations of the artificial gauges marked as "g". The area shown by a blue box in the left panel is enlarged in the right panel. **b** Simulated Waveforms from MVC-1, -2 and -3 at different locations

credibility and thus usability of the system. In contrast, the use of wave monitoring, both using coastal wave gauges and offshore gauges, are able to confirm if a tsunami has been triggered by the source (Bellotti et al., 2009). Dedicated tsunami wave recording systems may play a fundamental role in such systems, to favor the early detection of the tsunami. The automated triggering system in place at Stromboli was able to detect the 28 August 2019 tsunami just 24 s after the tsunami generation, that is approximately 15 s after the tsunami onset and 1 min and 15 s after the volcanic explosion (Selva et al., 2021). This would provide the possibility for timely triggering the warning system even in cases with short propagation times like Stromboli (Esposti Ongaro et al., 2021).

The short travel time of the waves to the threatened coasts and the absence of real-time monitoring systems make the implementation of forecasting capabilities for such tsunami events quite challenging (Omira et al., 2022a). Nevertheless, it should also be noted that in cases where the maximum inundation takes place much later than the initial tsunami arrival, the time window of the tsunami early warning increases due to the dispersive nature of the wave propagation along the coast (Bellotti et al., 2009). As the 15 January 2022 Tonga volcanic explosion and resulting tsunami demonstrated, early warning systems targeting volcanic-tsunamis should be formulated as multi-hazard early warning systems integrated into the regional tsunami warning systems. Such a system would be composed of local volcanic and sea-level monitoring capabilities (Andronico et al., 2021; Ripepe et al., 2021; Selva et al., 2021), seismic (La Rocca et al., 2004; Pino et al., 2004), GNSS (Cegla et al., 2022; Lee et al., 2015), infrasound (Matoza et al., 2014; Kurokawa et al., 2020;

Werner-Allen et al., 2005), hydroacoustic (Cecioni et al., 2014; Chadwick et al., 2012; Caplan-Auerbach et al., 2001; Caplan-Auerbach et al., 2014) and meteorological (Silvestri et al., 2019) sensors. This is in line with the target "g" of the Sendai Framework for Disaster Risk Reduction 2015–2030 (https://www.undrr.org/publication/sendai-framework-disaster-risk-reduction-2015-2030), which emphasizes the need to substantially increase the availability of and access to multi-hazard early warning systems and disaster risk information and assessments to people by 2030. Such systems should also make use of best practices of operational landslide early-warning systems around the globe (Baroñ et al., 2012; Bazin, 2012; Michoud et al., 2013; Cloutier et al., 2015; Calvello et al., 2017). It may be the right time to implement a local tsunami early warning system on the Santorini within the multi-hazard framework and integrate it to the Intergovernmental Coordination Group (ICG) for the Tsunami Early Warning and Mitigation System in the Northeastern Atlantic, the Mediterranean and connected seas (ICG/NEAMTWS).

5. Conclusion

Our study shows that the considered scenarios are able to generate significant local tsunamis impacting Santorini and the nearby islands, as well as producing considerable impact along the coasts of the Southern Aegean Sea. While maximum tsunami amplitudes/arrival time ranges are 1.2 m/30-90 min for locations in the Greek-Turkish coasts in the far field, they are in the order of ≈ 60 m/1-2 min for some locations at the Santorini Island. The extreme tsunami amplitudes and short arrival times for locations inside the Santorini Island are a major challenge in terms of tsunami hazard warning and mitigation. As the warning lead time is too short to allow any meaningful evacuation, possibly the only way to mitigate tsunami hazards at the Santorini Island is to encourage local residents to avoid construction and residence on the shore. Experiences from the 2018 Anak Krakatau tsunami disaster showed that a distance of at least 100 m from the coastline could save lives and properties (Heidarzadeh et al., 2020b).

Obviously, such a safe distance would be different from one region to another, and would depend on the characteristics of the coast and the tsunamigenesis of each zone. For the Santorini Island region, detailed tsunami modeling including inundation calculations and probabilistic scenarios are necessary to develop tsunami inundation maps for the region and to advise local people of the most dangerous tsunami zones.

Author Contributions The concept of the study and the first draft of the manuscript was prepared by ON. MH performed tsunami modeling based on the sources identified by GEV with the support of JS. All authors commented on previous versions and to the improvement of the manuscript. All authors read and approved the final manuscript.

Data Availability

All data used in this study are provided in the body of the article.

Declarations

Publisher's Note Springer Nature remains neutral with regard to jurisdictional claims in published maps and institutional affiliations.

References

Abadie, S., Harris, J. C., Grilli, S. T., & Fabre, R. (2012). Numerical modeling of tsunami waves generated by the flank collapse of the Cumbre Vieja Volcano (La Palma, Canary Islands): Tsunami source and near field effects. *Journal of Geophysical Research.* https://doi.org/10.1029/2011JC007646

Abadie, S., Paris, A., Ata, R., et al. (2020) La Palma landslide tsunami: Computation of the tsunami source with a calibrated multi-fluid Navier-Stokes model and wave impact assessment with propagation models of different types. *Natural Hazard and Earth System Sciences, 20*, 3019–3038. https://doi.org/10.5194/nhess-2019-225

Acocella, V., Di Lorenzo, R., Newhall, C., & Scandone, R. (2015). An overview of recent (1988 to 2014) caldera unrest: Knowledge and perspectives. *Reviews of Geophysics, 53*, 896–955. https://doi.org/10.1002/2015RG000492

Alexandri, M., Papanikolaou, D., Nomikou, P., Ballas, D. (2003). Santorini volcanic field. New insights based on swath bathymetry. *Proceedings of the IUGG conference*, Sapporo, Japan.

Andronico, D., Del Bello, E., D'Oriano, C., et al. (2021). Uncovering the eruptive patterns of the 2019 double paroxysm eruption crisis of Stromboli volcano. *Nature Communications, 12*, 4213. https://doi.org/10.1038/s41467-021-24420-1

Antoniou, V., Lappas, S., Leoussis, C. and Nomikou, P. (2017). Landslide risk assessment of the Santorini Volcanic Group. In *Proceedings of the 3rd International Conference on Geographical Information Systems Theory, Applications and Management (GISTAM 2017)*. p 131–141. https://doi.org/10.5220/0006385801310141

Aspinall, W. P., & Woo, G. (2014). Santorini unrest 2011–2012: An immediate Bayesian belief network analysis of eruption scenario probabilities for urgent decision support under uncertainty. *Journal of Applied Volcanology.* https://doi.org/10.1186/s13617-014-0012-8

Barberi, F., & Carapezza, M. L. (2019). Explosive volcanoes in the Mediterranean area: Hazards from future eruptions at Vesuvius (Italy) and Santorini (Greece). *Annals of Geophysics.* https://doi.org/10.4401/ag-7761

Barberi, F., Corrado, G., Innocenti, F., & Luongo, G. (1984). Phlegraean fields 1982–1984: Brief chronicle of a volcano emergency in a densely populated area. *Bulletin of Volcanology, 47*, 175–185. https://doi.org/10.1007/BF01961547

Baroñ I., Supper R., Ottowitz D. (2012). Report on Evaluation of Mass Movement Indicators. Project SafeLand "*Living With Landslide Risk in Europe: Assessment, Effects of Global Change, and Risk Management Strategies*", Deliverable 4.6, (https://www.ngi.no/eng/Projects/SafeLand. Retrieved: 22/3/2022).

Barreca, G., Gross, F., Scarfì, L., Aloisi, M., Monaco, C., & Krastel, S. (2021). The Strait of Messina: Seismotectonics and the source of the 1908 earthquake. *Earth-Science Reviews*. https://doi.org/10.1016/j.earscirev.2021.103685

Batzakis, D. V., Misthos, L. M., Voulgaris, G., et al. (2020). Assessment of building vulnerability to tsunami hazard in Kamari (Santorini Island, Greece). *Journal of Marine Science and Engineering, 8*, 886. https://doi.org/10.3390/jmse8110886

Bazin, S. (2012). Guidelines for landslide monitoring and early warning systems in Europe—Design and required technology. Project SafeLand "*Living With Landslide Risk in Europe: Assessment, Effects of Global Change, and Risk Management Strategies*", Deliverable 4.8. https://www.ngi.no/eng/Projects/SafeLand. Accessed 22/3/2022.

Behrens, J., Løvholt, F., Fatemeh, J., et al. (2021). Probabilistic tsunami hazard and risk analysis: A review of research gaps. *Frontiers in Earth Science*. https://doi.org/10.3389/feart.2021.628772

Beisel, S., Chubarov, L., Didenkulova, I., et al. (2009). The 1956 Greek tsunami recorded at Yafo, Israel, and its numerical modeling. *Journal of Geophysical Research, 114*, C09002. https://doi.org/10.1029/2008JC005262

Bell, K. L. C., Carey, S. N., Nomikou, P., Sigurdsson, H., & Sakellariou, D. (2013). Submarine evidence of a debris avalanche deposit on the eastern slope of Santorini volcano. *Greece, Tectonophysics, 597–598*, 147–160. https://doi.org/10.1016/j.tecto.2012.05.006

Bellotti, G., Di Risio, M., & De Girolamo, P. (2009). Feasibility of tsunami early warning systems for small volcanic islands. *NaturalHazards and Earth Systems Sciences, 9*, 1911–1919. https://doi.org/10.5194/nhess-9-1911-2009

Berndt, C., Brune, S., Nisbet, E., Zschau, J., & Sobolev, V. S. (2009). Tsunami modeling of a submarine landslide in the Fram Strait: Tsunami models for a landslide off Svalbard. *Geochemistry, Geophysics, Geosystems*. https://doi.org/10.1029/2008GC002292

Bonaccorso, A., Calvari, S., Garfì, G., Lodato, L., & Patanè, D. (2003). Dynamics of the December 2002 flank failure and tsunami at Stromboli volcano inferred by volcanological and geophysical observations. *Geophysical Research Letters*. https://doi.org/10.1029/2003GL017702

Bond, A., & Sparks, R. S. J. (1976). The Minoan eruption of Santorini, Greece. *Journal of Geological Society London, 132*, 1–16.

Borrero, J. C., Solihuddin, T., Fritz, H. M., Lynett, P. J., Prasetya, G. S., & Synolakis, C. E. (2020). Field survey and numerical modelling of the December 22, 2018 Anak Krakatau tsunami. *Pure and Applied Geophysics, 177*(6), 2457–2475. https://doi.org/10.1007/s00024-020-02515-y

Calvello, M. (2017). Early warning strategies to cope with landslide risk. *Rivista Italiana Di Geotecnica*. https://doi.org/10.19199/2017.2.0557-1405.063

Caplan-Auerbach, J., & Duennebier, F. K. (2001). Hydroacoustic detection of submarine landslides on Kilauea volcano. *Geophysical Research Letters, 28*(9), 1811–1813.

Caplan-Auerbach, J., Dziak, R. P., Bohnenstiehl, D. R., Chadwick, W. W., & Lau, T.-K. (2014). Hydroacoustic investigation of submarine landslides at West Mata volcano Lau Basin. *Geophysical Research Letters, 41*, 5927–5934. https://doi.org/10.1002/2014GL060964

Carey, S., Sigurdsson, H., Mandeville, C., Bronto, S. (1996). Pyroclastic flows and surges over water: an example from the 1883 Krakatau eruption. *Bulletin of Volcanology*, *57*, 493–511. https://doi.org/10.1007/BF00304435

Carey, S., Sigurdsson, H., Alexandri, M., et al. (2006). Submarine volcaniclastic deposits associated with the Minoan eruption of Santorini volcano Greece. *EOS Transactions, American Geophysical Union, 87*, 26.

Casagli, N., Tebaldi, A., Merri, A., et al. (2009). Deformation of Stromboli Volcano (Italy) during the 2007 crisis by radar interferometry, numerical modeling and field structural data. *Journal of Volcanology and Geothermal Research, 182*(3–4), 182–200. https://doi.org/10.1016/j.jvolgeores.2009.01.002

Cecioni, C., Bellotti, G., Romano, A., Abdolali, A., Sammarco, P., & Franco, L. (2014). Tsunami early warning system based on real-time measurements of hydro-acoustic waves. *Procedia Engineering, 70*, 311–320. https://doi.org/10.1016/j.proeng.2014.02.035

Cegla, A., Rohm, W., Lasota, E., & Biondi, R. (2022). Detecting volcanic plume signatures on GNSS signal, based on the 2014 Sakurajima Eruption. *Advances in Space Research, 69*(1), 292–307. https://doi.org/10.1016/j.asr.2021.08.034

Chadwick, W. W., Dziak, R. P., Haxel, J. H., Embley, R. W., & Matsumoto, H. (2012). Submarine landslide triggered by volcanic eruption recorded by in situ hydrophone. *Geology, 40*(1), 51–54. https://doi.org/10.1130/G32495.1

Charlton, D., Kilburn, C., & Edwards, S. (2020). Volcanic unrest scenarios and impact assessment at Campi Flegrei caldera, Southern Italy. *Journal of Applied Volcanology, 9*, 7. https://doi.org/10.1186/s13617-020-00097-x

Chouliaras, G., Drakatos, G., Makropoulos, K., & Melis, N. S. (2012). Recent seismicity detection increase in the Santorini volcanic island complex. *Natural Hazards and Earth Systems Sciences, 12*, 859–866. https://doi.org/10.5194/nhess-12-859-2012

Cloutier, C., Agliardi, F., Crosta, G. B., et al. (2015). The First International Workshop on Warning Criteria for Active Slides: Technical issues, problems and solutions for managing early warning systems. *Landslides, 12*(1), 205–212.

De Girolamo, P., Di Risi, M., Romano, A., & Molfetta, M. G. (2014). Landslide tsunami: Physical modeling for the implementation of tsunami early warning systems in the Mediterranean Sea. *Procedia Engineering., 70*, 429–438. https://doi.org/10.1016/j.proeng.2014.02.048

De Lange, W. P., Prasetya, G. S., & Healy, T. R. (2001). Modelling of tsunamis generated by pyroclastic flows (Ignimbrites). *Natural Hazards, 24*, 251–266.

Di Traglia, F., Nolesini, T., Intrieri, E., et al. (2014). Review of ten years of volcano deformations recorded by the ground-based InSAR monitoring system at Stromboli volcano: A tool to mitigate volcano flank dynamics and intense volcanic activity. *Earth-Science Reviews, 139*, 317–335. https://doi.org/10.1016/j.earscirev.2014.09.011

Dimitriadis, I., Karagianni, E., Panagiotopoulos, D. G., et al. (2009). Seismicity and active tectonics at Coloumbo Reef (Aegean Sea, Greece): Monitoring an active volcano at Santorini

Volcanic Center using a temporary seismic network. *Tectonophysics, 465*, 136–149. https://doi.org/10.1016/j.tecto.2008.11.005

Dipartimento della Protezione Civile and Regione Sicilia (2015). Isola di Stromboli—Piano nazionale di emergenza a fronte di eventi vulcanici di rilevanza nazionale, https://rischi.protezionecivile.gov.it/static/3b89029643532bdb10a49064c0504cc5/pianonazionalestromboli2015.pdf (in Italian) Last Accessed: 15 March 2023

Dogan, G. G., Annunziato, A., Hidayat, R., et al. (2021). Numerical simulations of December 22, 2018 Anak Krakatau tsunami and examination of possible submarine landslide scenarios. *Pure and Applied Geophysics, 178*, 1–20. https://doi.org/10.1007/s00024-020-02641-7

Dominey-Howes, D. (2004). A re-analysis of the Late Bronze Age eruption and tsunami of Santorini, Greece, and the implications for the volcano-tsunami hazard. *Journal of Volcanology and Geothermal Research, 130*, 107–132. https://doi.org/10.1016/S0377-0273(03)00284-1

Druitt, T. H., Edwards, L., Mellors, R. M., et al. (1999). Santorini volcano. *Memoir of the Geological Society of London, 19*, 176.

Druitt, T. H., & Francaviglia, V. (1992). Caldera formation on Santorini and the physiography of the islands in the late Bronze Age. *Bulletin of Volcanology, 54*, 484–493. https://doi.org/10.1007/BF00301394

Druitt, T. H., McCoy, F. W., & Vougioukalakis, G. E. (2019). The Late Bronze Age eruption of Santorini Volcano and its impact on the ancient mediterranean world. *Elements, 15*, 185–190.

Druitt, T. H., Mellors, R. A., Pyle, D. M., & Sparks, R. S. J. (1989). Explosive volcanism on Santorini Greece. *Geological Magazine., 126*, 95–126. https://doi.org/10.1017/S0016756800006270

EspostiOngaro, T., de MichieliVitturi, M., Cerminara, M., et al. (2021). Modeling tsunamis generated by submarine landslides at Stromboli volcano (Aeolian Islands, Italy): A numerical benchmark study. *Frontiers of Earth Science, 9*, 628652. https://doi.org/10.3389/feart.2021.628652

Favalli, M., Boschi, E., Mazzarini, F., & Pareschi, M. T. (2009). Seismic and landslide source of the 1908 Straits of Messina tsunami (Sicily, Italy). *Geophysical Research Letters., 36*, L16304. https://doi.org/10.1029/2009GL039135

Forte, G., De Falco, M., Santangelo, N., & Santo, A. (2019). Slope stability in a multi-hazard eruption scenario (Santorini, Greece). *Geosciences, 9*, 412. https://doi.org/10.3390/geosciences9100412

Francalanci, L., Vougioukalakis, G., Perini, G., & Manetti, P. (2005). A west–east traverse along the magmatism of the south Aegean volcanic arc in the light of volcanological, chemical and isotope data. In M. Fytikas & G. Vougioukalakis (Eds.), *The South Aegean active volcanic arc: Present knowledge and future perspectives: Developments in volcanology* (Vol. 7, pp. 65–111). Elsevier.

Freundt, A. (2003). Entrance of hot pyroclastic flows into the sea: Experimental observations. *Bulletin of Volcanology, 65*, 144–164. https://doi.org/10.1007/s00445-002-0250-1

Friedrich, W.L., Kromer, B., Friedrich, M., Heinemeier, J., Pfeiffer, T., Talamo, S. (2006). Santorini eruption radiocarbon dated to 1627–1600 B.C. *Science*. 312: 548. https://doi.org/10.1126/science.1125087.

Friedrich, W. (2000). *Fire in the sea, the Santorini volcano: Natural history and the legend of Atlantis*. Cambridge University Press.

Fritz, H. M., Hager, W. H., & Minor, H. E. (2004). Near field characteristics of landslide generated impulse waves. *Journal of Waterway, Port, Coastal, and Ocean Engineering, 130*(6), 287–302. https://doi.org/10.1061/(ASCE)0733-950X(2004)130:6(287)

Fu, L., Heidarzadeh, M., Cukur, D., et al. (2017). Tsunamigenic potential of a newly discovered active fault zone in the outer Messina Strait Southern Italy. *Geophysical Research Letters, 44*(5), 2427–2435. https://doi.org/10.1002/2017GL072647

Fytikas, M., Innocenti, F., Manetti, P., Peccerillo, A., Mazzuoli, R., & Villari, L. (1984). Tertiary to quaternary evolution of volcanism in the Aegean region. In J. E. Dixon & A. H. F. Robertson (Eds.), *The geological evolution of the Eastern Mediterranean* (Vol. 17, pp. 687–699). Special Publications of the Geological Society.

Fytikas, M., Kolios, N., & Vougioukalakis, G. E. (1990). Post-Minoan volcanic activity on the Santorini volcano. Volcanic hazard and risk. Forecasting possibilities. In D. A. Hardy, J. Keller, V. P. Galanopoulos, N. C. Flemming, & T. H. Druitt (Eds.), *Thera and the Aegean World III 2* (pp. 183–198). The Thera Foundation.

Georgalas, G. (1953). L'éruption du volcan de Santorini en 1950. *Bulletin of Volcanology, 13*, 39–55.

Georgalas, G. C. (1962). Active volcanoes in the world including solfatara fields. *International Association of Volcanology, 12*, 1–40.

Geshi, N., Maeno, F., Nakagawa, S., Naruo, H., & Kobayashi, T. (2017). Tsunami deposits associated with the 7.3 ka caldera-forming eruption of the Kikai Caldera, insights for tsunami generation during submarine caldera-forming eruptions. *Journal of Volcanology and Geothermal Research, 347*, 221–233. https://doi.org/10.1016/j.jvolgeores.2017.09.015

Giachetti, T., Paris, R., Kelfoun, K., & Ontowirjo, B. (2012). Tsunami hazard related to a flank collapse of Anak Krakatau volcano, Sunda Strait, Indonesia. In J. P. Terry & J. Goff (Eds.), *Natural hazards in the Asia—Pacific region: Recent advances and emerging concepts geological society* (Vol. 361, pp. 79–90). Special Publications. https://doi.org/10.1144/SP361.7

Goodman-Tchernov, B. N., Dey, H. W., Reinhardt, E. G., McCoy, F., & Mart, Y. (2009). Tsunami waves generated by the Santorini eruption reached Eastern Mediterranean shores. *Geology, 37*(10), 943–946. https://doi.org/10.1130/G25704A.1

Grezio, A., Babeyko, A., Baptista, M. A., et al. (2017). Probabilistic tsunami hazard analysis: Multiple sources and global applications. *Reviews of Geophysics, 55*, 1158–1198. https://doi.org/10.1002/2017RG000579

Grilli, S. T., Tappin, D. R., Carey, S., et al. (2019). Modelling of the tsunami from the December 22, 2018 lateral collapse of Anak Krakatau volcano in the Sunda Straits. *Indonesia. Scientific Reports, 9*(1), 1–13. https://doi.org/10.1038/s41598-019-48327-6

Grilli, S. T., Zhang, C., Kirby, J. T., et al. (2021). Modeling of the Dec. 22nd 2018 Anak Krakatau volcano lateral collapse and tsunami based on recent field surveys: Comparison with observed tsunami impact. *Marine Geology, 440*, 106566. https://doi.org/10.1016/j.margeo.2021.106566

Hasiotis, T., Papatheodorou, G., Charalampakis, M., Stefatos, A., & Ferentinos, G. (2007). High frequency sediment failures. In A submarine volcanic environment The Santorini (Thera) Basin In The Aegean Sea. In V. Lykousis, D. Sakellariou, & J. Locat (Eds.), *In The Aegean sea submarine mass movements and their consequences. Advances in natural and technological hazards research.* (Vol. 27). Springer. https://doi.org/10.1007/978-1-4020-6512-5_32

Hayes, J. L., Wilson, T. M., Deligne, N. I., et al. (2020). Developing a suite of multi-hazard volcanic eruption scenarios using an interdisciplinary approach. *Journal of Volcanology and Geothermal Research., 392*, 106763. https://doi.org/10.1016/j.jvolgeores.2019.106763

Heidarzadeh, M., Gusman, A., Ishibe, T., Sabeti, R., & Šepić, J. (2022). Estimating the eruption-induced water displacement source of the 15 January 2022 Tonga volcanic tsunami from tsunami spectra and numerical modelling. *Ocean Engineering, 261*, 112165. https://doi.org/10.1016/j.oceaneng.2022.112165

Heidarzadeh, M., Ishibe, T., Sandanbata, O., Muhari, A., & Wijanarto, A. B. (2020a). Numerical modeling of the subaerial landslide source of the 22 December 2018 Anak Krakatoa volcanic tsunami Indonesia. *Ocean Engineering, 195*, 106733. https://doi.org/10.1016/j.oceaneng.2019.106733

Heidarzadeh, M., & Kijko, A. (2011). A probabilistic tsunami hazard assessment for the Makran subduction zone at the northwestern Indian Ocean. *Natural Hazards, 56*(3), 577–593. https://doi.org/10.1007/s11069-010-9574-x

Heidarzadeh, M., Krastel, S., & Yalciner, A. C. (2014). The state-of-the-art numerical tools for modeling landslide tsunamis: A short review Chapter 43. *Submarine mass movements and their consequences* (pp. 483–495). Springer International publishing. https://doi.org/10.1007/978-3-319-00972-8_43 ISBN: 978-3-319-00971-1.

Heidarzadeh, M., Putra, P. S., & Nugroho, S. H. (2020b). Field survey of tsunami heights and runups following the 22 December 2018 Anak Krakatau volcano tsunami, Indonesia. *Pure and Applied Geophysics, 177*, 4577–4595. https://doi.org/10.1007/s00024-020-02587-w

Heidarzadeh, M., Rabinovich, A. B., Kusumoto, S., & Rajendran, C. P. (2020c). Field surveys and numerical modeling of the 26 December 2004 Indian Ocean tsunami in the area of Mumbai, west coast of India. *Geophysical Journal International*. https://doi.org/10.1093/gji/ggaa277

Heidarzadeh, M., & Satake, K. (2015). Source properties of the 17 July 1998 Papua New Guinea tsunami based on tide gauge records. *Geophysical Journal International, 202*(1), 361–369. https://doi.org/10.1093/gji/ggv145

Heidarzadeh, M., & Satake, K. (2017). A combined earthquake–landslide source model for the tsunami from the 27 November 1945 M w 8.1 Makran earthquake. *Bulletin of the Seismological Society of America, 107*(2), 1033–1040. https://doi.org/10.1785/0120160196

Heiken, G., & McCoy, F. (1984). Caldera development during the Minoan eruption, Thera, Cyclades Greece. *Journal of Geophysical Research, 89*(B10), 8441–8462. https://doi.org/10.1029/JB089iB10p08441

Jenkins, S. F., Barsotti, S., Hincks, T. H., et al. (2015). Rapid emergency assessment of ash and gas hazard for future eruptions at Santorini Volcano Greece. *Journal of Applied Volcanology*. https://doi.org/10.1186/s13617-015-0033-y

Johnston, D., Scott, B. J., Houghton, B., et al. (2002). Social and economic consequences of historic caldera unrest at the Taupo volcano, New Zealand and the management of future episodes of unrest. *Bulletin of the New Zealand Society for Earthquake Engineering, 35*(4), 215–230. https://doi.org/10.5459/bnzsee.35.4.215-230

Jolivet, L., Faccenna, C., Huet, B., et al. (2013). Aegean tectonics: strain localisation, slab tearing and trench retreat. *Tectonophysics, 597–598*, 1–33. https://doi.org/10.1016/j.tecto.2012.06.011

Kaye, G., Cole, J., King, A., & Johnston, D. (2009). Comparison of risk from pyroclastic density current hazards to critical infrastructure in Mammoth Lakes, California, USA, from a new Inyo craters rhyolite dike eruption versus a dacitic dome eruption on Mammoth Mountain. *Natural Hazards, 49*(3), 541–563. https://doi.org/10.1007/s11069-009-9465-1

Kazantzidou-Firtinidou, D., Kassaras, I., & Ganas, A. (2018). Empirical seismic vulnerability, deterministic risk and monetary loss assessment in Fira (Santorini, Greece). *Natural Hazards, 93*, 1251–1275. https://doi.org/10.1007/s11069-018-3350-8

Kelfoun, K., Giachetti, T., & Labazuy, P. (2010). Landslide-generated tsunamis at Reunion Island. *Journal Geophysical Research Earth Surface*. https://doi.org/10.1029/2009jf001381

Krastel, S., Schmincke, H.-U., Jacobs, C. L., Rihm, R., Le Bas, T. P., & Alibés, B. (2001). Submarine landslides around the Canary Islands. *Journal of Geophysical Research: Solid Earth 106*, 3977–3997. https://doi.org/10.1029/2000JB900413

Kurokawa, A. K., & Ichihara, M. (2020). Identification of infrasonic and seismic components of tremors in single-station records: Application to the 2013 and 2018 events at Ioto Island, Japan. *Earth, Planets and Space, 72*, 171. https://doi.org/10.1186/s40623-020-01302-2

La Rocca, M., Galluzzo, D., Saccorotti, G., Tinti, S., Cimini, G. B., & Del Pezzo, E. (2004). Seismic signals associated with landslides and with a tsunami at Stromboli Volcano. *Italy, Bulletin of the Seismological Society of America, 94*, 1850–1867. https://doi.org/10.1785/012003238

Lacanna, G. and Ripepe M. (2020). Genesis of tsunami waves generated by Pyroclastic flows and the Early-Warning system, *Abstract 4a Conferenza A. Rittmann*, Catania (2020).

Lavigne, F., Julie, M., Patrick, W., et al. (2021). Bridging legends and science: Field evidence of a large tsunami that affected the Kingdom of Tonga in the 15th Century. *Frontiers in Earth Science*. https://doi.org/10.3389/feart.2021.748755

Le Pichon, X., & Angelier, J. (1979). The Hellenic arc and trench system: A key to the neotectonic evolution of the eastern Mediterranean area. *Tectonophysics, 60*, 1–42. https://doi.org/10.1016/0040-1951(79)90131-8

Lee, S.-W., Yun, S.-H., Kim, D. H., Lee, D., Lee, Y. J., & Schutz, B. E. (2015). Real-time volcano monitoring using GNSS single-frequency receivers. *Journal of GeophysicalResearch Solid Earth, 120*, 8551–8569. https://doi.org/10.1002/2014JB011648

Longo, M. L. (2019). How memory can reduce the vulnerability to disasters: The bradyseism of Pozzuoli in southern Italy. *AIMS Geosciences, 5*(3), 631–644. https://doi.org/10.3934/geosci.2019.3.631

Løvholt, F., Glimsdal, S., & Harbitz, C. B. (2020). On the landslide tsunami uncertainty and hazard. *Landslides, 17*, 2301–2315. https://doi.org/10.1007/s10346-020-01429-z

Mani, L., Tzachor, A., & Cole, P. (2021). Global catastrophic risk from lower magnitude volcanic eruptions. *Nature Communications, 12*, 4756. https://doi.org/10.1038/s41467-021-25021-8

Manning, S. W., Ramsey, C. B., Kutschera, W., et al. (2006). Chronology for the Aegean Late Bronze Age 1700–1400 B.C. *Science, 312*, 565–569. https://doi.org/10.1126/science.1125682

Maramai, A., Brizuela, B., & Graziani, L. (2014). The euro-mediterranean tsunami catalogue. *Annals of Geophysics, 57*(4), 0435. https://doi.org/10.4401/ag-6437

Maramai, A., Graziani, L., & Tinti, S. (2005). Tsunamis in the Aeolian Islands (southern Italy): A review. *Marine Geology, 215*(1–2), 11–21. https://doi.org/10.1016/j.margeo.2004.03.018

Matoza, R. S., & Fee, D. (2014). Infrasonic component of volcano-seismic eruption tremor. *Geophyical Research Letters, 41,* 1964–1970. https://doi.org/10.1002/2014GL059301

McCoy, F., & Heiken, G. (2000). Tsunami generated by the Late Bronze Age eruption of Thera (Santorini) Greece. *Pure and Applied Geophysics., 157,* 1227–1256. https://doi.org/10.1007/s000240050024

McCoy, F., Synolakis, C. E., & Papadopoulos, G. A. (2000). Tsunami generated during the LBA eruption of thera—Evidence from modelling and sedimentary deposits. *EOS Transactions American Geophysical Union, 81,* T21E–T13.

McFall, B. C., & Fritz, H. M. (2016). Physical modelling of tsunamis generated by three-dimensional deformable granular landslides on planar and conical island slopes. *Proceedings of the Royal Society a: Mathematical, Physical and Engineering Sciences, 472*(2188), 20160052. https://doi.org/10.1098/rspa.2016.0052

McKenzie, D. P. (1970). Plate tectonics of the Mediterranean region. *Nature, 226,* 239–243. https://doi.org/10.1038/226239a0

McKenzie, D. P. (1972). Active tectonics of the Mediterranean region. *Geophys Journal of the Royal Astronomical Society, 30,* 109–185. https://doi.org/10.1111/j.1365-246X.1972.tb02351.x

McKenzie, D. P. (1978). Active Tectonics of the Alpine-Himalayan Belt: The Aegean Sea and Surrounding Regions. *Geophysical Journal of the Royal Astronomical Society, 55,* 217–254. https://doi.org/10.1111/j.1365-246X.1978.tb04759.x

Michoud, C., Bazin, S., Blikra, L. H., Derron, M. H., & Jaboyedoff, M. (2013). Experiences from site-specific landslide early warning systems. *Natural Hazards and Earth System Sciences, 13*(10), 2659–2673. https://doi.org/10.5194/nhess-13-2659-2013

Minoura, K., Imamura, F., Kuran, U., et al. (2000). Discovery of Minoan tsunami deposits. *Geology, 28*(1), 59–62. https://doi.org/10.1130/0091-7613(2000)028%3c0059:DOMTD%3e2.0.CO;2

Moratto, L., Orlecka-Sikora, B., Costa, G., Suhadolc, P., Papaioannou, C., & Papazachos, C. B. (2007). A deterministic seismic hazard analysis for shallow earthquakes in Greece. *Tectonophysics, 442,* 66–82. https://doi.org/10.1016/j.tecto.2007.05.004

Necmioglu, O., & Ozel, N. M. (2015). Earthquake Scenario-based tsunami wave heights in the eastern Mediterranean and Connected Seas. *Pure and Applied Geophysics, 172*(12), 3617–3638.

Necmioğlu, Ö., Turhan, F., Özer Sözdinler, C., et al. (2021). KOERI's tsunami warning system in the Eastern Mediterranean and its Connected Seas: A decade of achievements and challenges. *Applied Sciences, 11,* 11247. https://doi.org/10.3390/app112311247

Newhall, C. G., Dzurisin, D. (1988). *Historical unrest at large calderas of the world.* U.S., G.P.O. Bulletin 1855. 2: 1108

Newman, A. V., Stiros, S., Feng, L., et al. (2012). Recent geodetic unrest at Santorini Caldera, Greece. *Geophysical Research Letters, 39,* L06309. https://doi.org/10.1029/2012GL051286

Nishimura, Y., Shiki, T. S., Tsuji, Y., Yamazako, T., & Minoura, K. (2008). *Tsunamiites features and implications* (pp. 163–184). Elsevier.

Nomikou, P., Carey, S., Bell, K. L. C., et al. (2014). Tsunami hazard risk of a future volcanic eruption of Kolumbo submarine volcano, NE of Santorini Caldera, Greece. *Natural Hazards, 72,* 1375–1390. https://doi.org/10.1007/s11069-012-0405-0

Nomikou, P., Carey, S., Papanikolaou, D., et al. (2012). Submarine volcanoes of the Coloumbo volcanic zone NE of Santorini Caldera, Greece. *Global and Planetary Change, 90–91,* 135–151. https://doi.org/10.1016/j.gloplacha.2012.01.001

Nomikou, P., Druitt, T. H., Hübscher, C., et al. (2016). Post-eruptive flooding of Santorini caldera and implications for tsunami generation. *Nature Communications, 7,* 13332. https://doi.org/10.1038/ncomms13332

Okal, E. A., & Synolakis, C. E. (2004). Source discriminants for near-field tsunamis. *Geophysical Journal International, 158*(3), 899–912. https://doi.org/10.1111/j.1365-246X.2004.02347.x

Okal, E. A., Synolakis, C. E., Uslu, B., Kalligeris, N., & Voukouvalas, E. (2009). The 1956 earthquake and tsunami in Amorgos Greece. *Geophysical Journal International, 178*(3), 1533–1554. https://doi.org/10.1111/j.1365-246X.2009.04237.x

Omira, R., Baptista, M. A., Quartau, R., et al. (2022a). How hazardous are tsunamis triggered by small-scale mass-wasting events on volcanic islands? New insights from Madeira—NE Atlantic. *Earth and Planetary Science Letters.* https://doi.org/10.1016/j.epsl.2021.117333

Omira, R., Ramalho, R. S., Kim, J., et al. (2022b). Global Tonga tsunami explained by a fast-moving atmospheric source. *Nature.* https://doi.org/10.1038/s41586-022-04926-4

Papazachos, B. C. (1990). Seismicity of the Aegean and surrounding area. *Tectonophysics, 178,* 287–308. https://doi.org/10.1016/0040-1951(90)90155-2

Papazachos, B. C., & Comninakis, P. E. (1971). Geophysical and tectonic features of the Aegean arc. *Journal of Geophysical Research, 76,* 8517–8533. https://doi.org/10.1029/jb076i035p08517

Pararas-Carayannis, G. (2002). Evaluation of the Threat of Mega Tsunami Generation from Postulated Massive Slope Failures of Island Stratovolcanoes on La Palma Canary Islands, and on the Island of Hawaii. *Science of Tsunami Hazards, 20*(5), 251–277.

Paris, R. (2015). Source mechanisms of volcanic tsunamis. *Philosophical Transactions of the Royal Society.* https://doi.org/10.1098/rsta.2014.0380

Paris, R., Switzer, A. D., Belousova, M., Belousov, A., Ontowirjo, B., Whelley, P. L., & Ulvrove, M. (2014). Volcanic tsunami: A review of source mechanisms, past events and hazards in Southeast Asia (Indonesia, Philippines, Papua New Guinea). *Natural Hazards, 70,* 447–470. https://doi.org/10.1007/s11069-013-0822-8

Parks, M. M., Moore, J. D. P., Papanikolaou, X., et al. (2015). From quiescence to unrest: 20 years of satellite geodetic measurements at Santorini volcano, Greece. *Journal of Geophysical Research Solid Earth, 120,* 1309–1328. https://doi.org/10.1002/2014JB011540

Perttu, A., Caudron, C., Assink, J. D., et al. (2020). Reconstruction of the 2018 tsunamigenic flank collapse and eruptive activity at Anak Krakatau based on eyewitness reports, seismo-acoustic and satellite observations. *Earth and Planetary Science Letters.* https://doi.org/10.1016/j.epsl.2020.116268

Phillipson, G., Sobradelo, R., & Gottsmann, J. (2013). Global volcanic unrest in the 21st century: An analysis of the first decade. *Journal of Volcanology and Geothermal Research, 264,* 183–196. https://doi.org/10.1016/j.jvolgeores.2013.08.004

Pichler, H., & Kussmaul, S. (1980). Comments on the geological map of the Santorini islands. In C. Doumas (Ed.), *Thera and the Aegean World II* (pp. 413–427). The Thera Foundation.

Pino, N. A., Ripepe, M., & Cimini, G. B. (2004). The Stromboli volcano landslides of December 2002: A seismological description. *Geophysical Research Letters., 31*, L02605. https://doi.org/10.1029/2003GL018385

Potter, S. H., Scott, B. J., Jolly, G. E., Johnston, D. M., & Neall, V. E. (2015). A catalogue of caldera unrest at Taupo Volcanic Centre, New Zealand, using the volcanic unrest index (VUI). *Bulletin of Volcanology, 77*(9), 78. https://doi.org/10.1007/s00445-015-0956-5

Pranantyo, I. R., Heidarzadeh, M., & Cummins, P. R. (2021). Complex tsunami hazards in eastern Indonesia from seismic and non-seismic sources: Deterministic modelling based on historical and modern data. *Geoscience Letters, 8*, 20. https://doi.org/10.1186/s40562-021-00190-y

Pyle, D. M. (1990). New estimates for the volume of the Minoan eruption. In D. A. Hardy, J. Keller, V. P. Galanopoulos, N. C. Flemming, & T. H. Druitt (Eds.), *Thera and the Aegean World III* (Vol. 2, pp. 113–121). The Thera Foundation.

Ripepe, M., Lacanna, G., Pistolesi, M., et al. (2021). Ground deformation reveals the scale-invariant conduit dynamics driving explosive basaltic eruptions. *Nature Communications, 12*, 1683. https://doi.org/10.1038/s41467-021-21722-2

Rizzo, A. L., Barberi, F., Carapezza, M. L., et al. (2015). New mafic magma refilling a quiescent volcano: Evidence from He-Ne-Ar isotopes during the 2011–2012 unrest at Santorini, Greece. *Geochemistry, Geophysics, Geosystems, 16*, 798–814.

Şahoğlu, V., Sterba, J. H., Katz, T., et al. (2022). Volcanic ash, victims, and tsunami debris from the Late Bronze Age Thera eruption discovered at Çeşme-Bağlararası (Turkey). *Proceedings of the National Academy of Sciences.* https://doi.org/10.1073/pnas.2114213118

Sahoo, S., Tiwari, D. K., Panda, D., & Kundu, B. (2022). Eruption cycles of Mount Etna triggered by seasonal climatic rainfall. *Journal of Geodynamics.* https://doi.org/10.1016/j.jog.2021.101896

Sakellariou, D., Sigurdsson, H., Alexandri, M., et al. (2010). Active tectonics in the Hellenic Volcanic Arc: The Coloumbo submarine volcanic zone. *Bulletin of the Geological Society of Greece., XLIII*2, 1056–1063.

Satake, K., Heidarzadeh, M., Quiroz, M., & Cienfuegos, R. (2020). History and features of trans-oceanic tsunamis and implications for paleo-tsunami studies. *Earth-Science Reviews., 202*, 103112. https://doi.org/10.1016/j.earscirev.2020.103112

Satow, C., Gudmundsson, A., Gertisser, R., et al. (2021). Eruptive activity of the Santorini volcano controlled by sea-level rise and fall. *Nature Geoscience., 14*, 586–592. https://doi.org/10.1038/s41561-021-00783-4

Selva, J., Acocella, V., Bisson, M., et al. (2019). Multiple natural hazards at volcanic islands: A review for the Ischia volcano (Italy). *Journal of Applied Volcanology, 8*, 5. https://doi.org/10.1186/s13617-019-0086-4

Selva, J., Amato, A., Armigliato, A., et al. (2021). Tsunami risk management for crustal earthquakes and non-seismic sources in Italy; Tsunami risk management for crustal earthquakes and non-seismic sources in Italy. *La Rivista Del Nuovo Cimento., 44*, 69–144. https://doi.org/10.1007/s40766-021-00016-9

Selva, J., Bonadonna, C., Branca, S., et al. (2020). Multiple hazards and paths to eruptions: A review of the volcanic system of Vulcano (Aeolian Islands, Italy). *Earth-Science Reviews., 207*, 103186. https://doi.org/10.1016/j.earscirev.2020.103186

Sigurdsson, H., & Carey, S. (1989). Plinian and co-ignimbrite tephra fall from the 1815 eruption of Tambora volcano. *Buletin of Volcanology, 51*(243–270), 84. https://doi.org/10.1007/BF01073515

Sigurdsson, H., Carey, S., Mandeville, C., & Bronto, S. (1991). Pyroclastic flows of the 1883 Krakatau eruption. *EOS Transactions, American Geophysical Union, 72*, 380–381.

Silvestri, M., Rabuffi, F., Pisciotta, A., et al. (2019). Analysis of thermal anomalies in volcanic areas using multiscale and multitemporal monitoring: Vulcano island test case. *Remote Sensing, 11*, 134. https://doi.org/10.3390/rs11020134

Sparks, R. S. J., & Wilson, C. J. N. (1990). The Minoan deposits: An overview of their characteristics and interpretation. In D. A. Hardy, J. Keller, V. P. Galanopoulos, N. C. Flemming, & T. H. Druitt (Eds.), *Thera and the Aegean World III* (Vol. 2, pp. 89–99). The Thera Foundation.

Stiros, S. C., Psimoulis, P., Vougioukalakis, G., & Fytikas, M. (2010). Geodetic evidence and modeling of a slow, small-scale inflation episode in the Thera (Santorini) volcano caldera. *Aegean Sea, Tectonophysics, 494*, 180–190. https://doi.org/10.1016/j.tecto.2010.09.015

Synolakis, C. E., Bardet, J. P., Borrero, J. C., et al. (2002). The slump origin of the 1998 Papua New Guinea tsunami. *Proceedings of the Royal Society of London. Series a: Mathematical, Physical and Engineering Sciences., 458*, 763–789. https://doi.org/10.1098/rspa.2001.0915

Tappin, D. R., Watts, P., & Grilli, S. T. (2008). The Papua New Guinea tsunami of 17 July 1998: Anatomy of a catastrophic event. *Natural Hazards and Earth System Sciences, 8*(2), 243–266. https://doi.org/10.5194/nhess-8-243-2008

Tassi, F., Vaselli, O., Papazachos, C. B., et al. (2013). Geochemical and isotopic changes in the fumarolic and submerged gas discharges during the 2011–2012 unrest at Santorini caldera (Greece). *Bulletin of Volcanology., 75*, 71. https://doi.org/10.1007/s00445-013-0711-8

Tinti, S., Manucci, A., Pagnoni, G., Armigliato, A., and Zaniboni, F. (2005). The 30 December 2002 landslide-induced tsunamis in Stromboli: sequence of the events reconstructed from the eyewitness accounts. *Natural Hazards and Earth Systems Sciences.* 5: 763–775. http://www.nat-hazards-earth-syst-sci.net/5/763/2005/.

Tinti, S., Pagnoni, G., & Zaniboni, F. (2006). The landslides and tsunamis of the 30th of December 2002 in Stromboli analysed through numerical simulations. *Bulletin of Volcanology, 68*(5), 462–479. https://doi.org/10.1007/s00445-005-0022-9

Titov, V. V. (2021). Hard Lessons of the 2018 Indonesian Tsunamis. *Pure Applied Geophysics, 178*, 1121–1133. https://doi.org/10.1007/s00024-021-02731-0

Valade, S., Lacanna, G., et al. (2016). Tracking dynamics of magma migration in open-conduit systems. *Bulletin of Volcanology.* https://doi.org/10.1007/s00445-016-1072-x

Vougioukalakis G., Sparks R.S.J., Pyle D., et al. (2016). Volcanic Hazard Assessment at Santorini Volcano: A Review and A Synthesis in the Light of the 2011–2012 Santorini Unrest, *Bulletin of the Geological Society of Greece*, L. Proceedings of the 14th International Congress, Thessaloniki. p. 274–283

Vougioukalakis, G. E., Francalanci, L., Sbrana, A., & Mitropoulos, D. (1995). The 1649–1650 Coloumbo submarine volcano activity, Santorini, Greece. In F. Barberi, R. Casale, & M. Fratta (Eds.), *The European laboratory volcanoes, workshop*

proceeding (pp. 189–192). European Commission European Science Foundation.

Vougioukalakis, G. E., & Fytikas, M. (2005). Volcanic hazards in the Aegean area, relative risk evaluation, monitoring and present state of the active volcanic centers. In M. Fytikas & G. Vougioukalakis (Eds.), *The South Aegean active volcanic arc: Present knowledge and future perspectives: Developments in volcanology* (Vol. 7, pp. 161–183). Elsevier.

Vougioukalakis, G. E., Mitropoulos, D., Perissoratis, C., Andrinopoulos, A., & Fytikas, M. (1994). The submarine volcanic centre of Coloumbo, Santorini, Greece. *Bulletin of the Geological Society of Greece, 3*, 351–360.

Vougioukalakis, G. E., Satow, C. G., & Druitt, T. H. (2019). Volcanism of the South Aegean Volcanic Arc. *Elements, 15*, 159–164.

Walter, T. R., Haghighi, M. H., Schneider, F. M., et al. (2019). Complex hazard cascade culminating in the Anak Krakatau sector collapse. *Nature Communications., 10*, 4339. https://doi.org/10.1038/s41467-019-12284-5

Wang, X., & Liu, P. L. F. (2006). An analysis of 2004 Sumatra earthquake fault plane mechanisms and Indian Ocean tsunami. *Journal of Hydraulic Research, 44*(2), 147–154.

Ward, S. N., & Day, S. (2001). Cumbre Vieja Volcano-Potential collapse and tsunami at La Palma, Canary Islands. *Geophysical Research Letters, 28*(17), 3397–3400. https://doi.org/10.1029/2001GL013110

Ward, S. N., & Day, S. (2003). Ritter Island Volcano - lateral collapse and the tsunami of 1888. *Geophysical Journal International, 154*, 891–902. https://doi.org/10.1046/j.1365-246X.2003.02016.x

Weatherall, P., Marks, K. M., Jakobsson, M., et al. (2015). A new digital bathymetric model of the world's oceans. *Earth and Space Science, 2*, 331–345. https://doi.org/10.1002/2015EA000107

Werner-Allen, G., Johnson, J., Ruiz, M., Lees, J., and Welsh, M. (2005). Monitoring volcanic eruptions with a wireless sensor network." *Proceeedings of the Second European Workshop on Wireless Sensor Network.* pp 108–120.

Wessel, P., & Smith, W. H. F. (1998). New, improved version of generic mapping tools released. *EOS, Transactions, American Geophysical Union, 79*(47), 579.

Ye, L., Kanamori, H., Rivera, L., Lay, T., Zhou, Y., Sianipar, D., & Satake, K. (2020). The 22 December 2018 tsunami from flank collapse of Anak Krakatau volcano during eruption. *Science Advances, 6*, 3. https://doi.org/10.1126/sciadv.aaz1377

Zengaffinen, T., Løvholt, F., Pedersen, G. K., & Muhari, A. (2020). Modelling 2018 Anak Krakatoa Flank Collapse and Tsunami: Effect of landslide failure mechanism and dynamics on tsunami generation. *Pure and Applied Geophysics, 177*(6), 2493–2516. https://doi.org/10.1007/s00024-020-02489-x

Zuccaro, G., Cacace, F., Spence, R. J. S., & Baxter, P. J. (2008). Impact of explosive eruption scenarios at Vesuvius. *Journal of Volcanolology and Geothermal Research, 178*(3), 416–453. https://doi.org/10.1016/j.jvolgeores.2008.01.005